

Soft medical microrobots: Design components and system integration

Cite as: Appl. Phys. Rev. **6**, 041305 (2019); doi: [10.1063/1.5124007](https://doi.org/10.1063/1.5124007)

Submitted: 12 August 2019 · Accepted: 1 October 2019 ·

Published Online: 22 October 2019



View Online



Export Citation



CrossMark

Rachel D. Field,^{a)}  Priya N. Anandakumaran,^{a)}  and Samuel K. Sia^{b)} 

AFFILIATIONS

Department of Biomedical Engineering, Columbia University, 351 Engineering Terrace, 1210 Amsterdam Avenue, New York, New York 10027, USA

^{a)}Contributions: R. D. Field and P. N. Anandakumaran contributed equally to this work.

^{b)}Author to whom correspondence should be addressed: ss2735@columbia.edu. Fax: (+1) 212-854-8725.

ABSTRACT

Medical microrobots are distinguished from other robotic systems in that they must function in the human body. As such, they exhibit special characteristics of size, function, and material choice. Recent advances have focused on fabrication techniques, locomotion at microscale environment, and targeted drug delivery. In this article, we will review these advances and examine related developments in material science and strategies for wireless control systems for communication, as well as data acquisition and processing. We focus on medical microrobots made of soft materials (with an emphasis on polymers and hydrogels), which are mechanically robust and deformable, offer tunable biophysical properties, and are highly biocompatible. Integration of the four design elements of locomotion, feedback and control, functionality, and biocompatibility will be needed to develop a fully functioning medical microrobot with clinical utility in the human body, such as diagnostics and treatment of disease, maintenance of wellness, and improvement of overall performance.

Published under license by AIP Publishing. <https://doi.org/10.1063/1.5124007>

TABLE OF CONTENTS

I. INTRODUCTION	1
II. DESIGN COMPONENTS	2
A. Locomotion	2
1. Within a liquid	3
2. At tissue boundaries	5
3. In swarms	6
4. Summary	6
B. Feedback and control	6
1. Extracorporeal controller	6
2. Intrinsic controller	10
C. Functionality	10
1. Sensing	10
2. Delivery of drugs and small molecules	11
3. Delivery of cells and large cargo	11
4. Microgrippers	11
D. Biocompatibility	11
1. Mechanical compatibility	12
2. Porosity	12
3. Degradability	13
4. Geometry and size	13
5. Other components within MMRs	13

III. SYSTEM INTEGRATION	13
IV. FUTURE PERSPECTIVES AND CONCLUSION	16

I. INTRODUCTION

For over half a century,^{1–3} there existed a fascination with microscopic robots swimming in the body—sensing signals, destroying unwanted cells, and repairing wounds. In recent years, important advances in different aspects for such a device have been made, including fabrication techniques and design for different sites within the body^{4,5} and, in particular, strategies for locomotion in propelling such devices.^{4,6} These developments, as well as research in related areas including wireless communication and material science, present an opportunity to consider how such devices, as a whole, could function. In this article, we will review recent advances in medical microrobots (MMRs), examine the necessary design elements including the relevant physics, and consider the path forward for building an integrated, fully functioning MMR with demonstrated clinical utility.

What are MMRs? Although not yet a standardized term, they have been referenced as small devices, from a millimeter to a few microns, that can travel through the human body and perform designed functions.^{3,4,7} Because MMRs must be appropriately small and biocompatible to function inside a human body, they exhibit

distinguishing features of size, functionality, and material choice compared to other types of robotics. First, most current work toward integrated MMRs assume proportions on the order of microscale (i.e., between $1\ \mu\text{m}$ and several millimeters, but primarily between 100 and $1000\ \mu\text{m}$). Although early conceptions of MMRs hypothesized nanoscale dimensions,^{1,8} nanoscale MMRs currently emphasize the design of molecular motors rather than a collective ability for sensing, actuation, computation, power storage, and communication.^{9–11} Second, MMRs are distinguished by their intended function in the human body, which include highly sensitive and precise diagnosis and treatment of disease, and general enhancement of human wellness and performance. By contrast, microrobots as a whole could find important use across a wide spectrum of settings, including outside the body for applications in sensing, energy, and molecular assembly.^{11,12} For medical use, compared to medical robotic systems that use macroscale tools for surgical assistance, MMRs could reach regions of the body (for example, via the circulatory or nervous system) that have traditionally been challenging for surgery, therapeutic delivery, or targeted diagnostics.¹³ For example, certain regions in the body (such as kidney, retina, and a growing fetus) that endure severe damage to protective tissues with traditional surgery still necessitate limited degrees of freedom (DOF) for laparoscopic surgery.^{14–16} At the intended site of intervention, MMRs could act as a temporary mechanical object (e.g., stent for cardiac vessel repairs^{17,18}), sense local biochemical or biophysical cues (e.g., to measure pressure intraocularly or within risk blood vessel^{19–21}), deliver precise localized doses of drugs (e.g., for retina treatments²²), or serve as a targeted tissue scaffold for cell therapy.²³

MMRs can be made of different materials. Taking a cue from macroscale electronic devices are microelectronic devices and robots, such as digestible smart pills through the gut.^{24–28} At the other end of the spectrum are biohybrid-based microdevices, which use living cells as actuation or locomotion elements.^{29–31} In this review, we focus on MMRs made of soft materials, which exhibit moduli in the range of the moduli of biological materials¹¹ and can be engineered to be biocompatible and for precise uses. For example, in applications outside the human body, soft robots—made with materials ranging from alginate, silicone, polydimethylsiloxane (PDMS), and rubber (all with elastic moduli at less than 1 GPa)^{11,32}—can exhibit high degrees of flexibility and agility. For MMRs inside the human body, soft materials are deformable (with similar elastic and rheological properties similar to biological tissue) and can recover their shape after passing through a constriction and, most importantly, can be tuned to be highly biocompatible over the intended intervention duration³³ to reduce damage to the surrounding tissue. Types of soft materials for MMRs include polymers, hydrogels, and proteins.^{5,34} In particular, hydrogels—which are three-dimensional, crosslinked polymeric networks with a high-water content—offer highly versatile and tunable properties (including diffusive and optical³⁵) and can be made to be stimuli-responsive;³⁶ although their benefits in the past had come at the expense of mechanical robustness, recent developments in composition and fabrication, including works from our group, have enhanced the mechanical properties (including elastic moduli and stretchability) of hydrogel-based structures to diversify their potential use and functionality.^{37–39}

This review will focus on the design elements and path forward for systems integration of an MMR toward successful *in vivo* use. Section II will discuss the necessary design elements of an MMR,

beginning with mechanisms for locomotion and feedback and control, and progressing to tissue-specific functionality and biocompatibility (Fig. 1). Section III will highlight recent examples that have attempted to integrate these elements toward whole MMRs and note areas for further research opportunities. Section IV will conclude with a discussion of the path forward for systems integration toward clinical use.

II. DESIGN COMPONENTS

A. Locomotion

Mechanisms to enable the locomotion of microrobots have been a focal point for researchers.^{2,4,29} Microrobots must have sufficient propulsion force and dexterity to reach their intended application site (Fig. 2). For devices to move at the microscale, they must successfully operate in an environment of low Reynolds number, where viscous forces have a more significant effect than occurs on the macroscale.^{40,41} The Reynolds number (Re) is defined as

$$Re = \frac{Lv\rho}{\eta}, \quad (1)$$

with kinematic velocity v , density ρ , length L , and viscosity η ; Re is the ratio of inertial to viscous fluids in the flow.⁴² The Reynolds number at the microscale is very low due to the small characteristic length and velocity such that the Navier-Stokes equation for such a system

$$\rho \frac{\partial \mathbf{u}}{\partial t} + \rho \mathbf{u} \cdot \nabla \mathbf{u} = -\nabla P + \eta \nabla^2 \mathbf{u} \quad (2)$$

can be simplified because the system's inertia and the acceleration of fluid can be considered negligible, resulting in a time-independent expression

$$0 = -\nabla P + \eta \nabla^2 \mathbf{u}, \quad (3)$$

where ∇P is the pressure gradient acting on fluid from nonuniform pressure, and $\eta \nabla^2 \mathbf{u}$ is the viscous term demonstrating the shear stress on fluid and opposing occurring motion.⁴³ For the design of MMRs, the significance of this simplification of the Navier-Stokes equation is that all time-dependent elements of motion are negligible, and therefore reciprocal motion does not translate into a functional strategy for motion. This principle can be best visualized according to Purcell's "scallop theorem": as a scallop only has a single hinge, it functions with a single degree of freedom and relies entirely dependent on reciprocal motion, which would render it incapable of motion if scaled down to the microscale.^{4,43} In these time-independent conditions, where all fluid essentially acts laminar along the surface of the device, motion must occur due to a nonreciprocal shape change; movement methods that rely on underlying inertial forces and reciprocal motions for propulsion, such as rigid oars or fishlike actuators, cannot effectively function [Fig. 2(a)].⁴⁴

While macroscale devices are primarily affected by inertia or weight, microscale devices are influenced more by surface effects and viscous forces.⁴ Previous reviews have classified designs for the locomotion of microrobots (e.g., Nelson and co-workers noting actuated appendages, flexible joints, catalytic conversion of chemical energy, soft microrobots, stimuli-responsive movement⁵). This section will focus on an analysis of movement of MMRs with simple and idealized geometry, with the relevant forces dependent upon the targeted location in the human body (Table I); we consider both whole-device

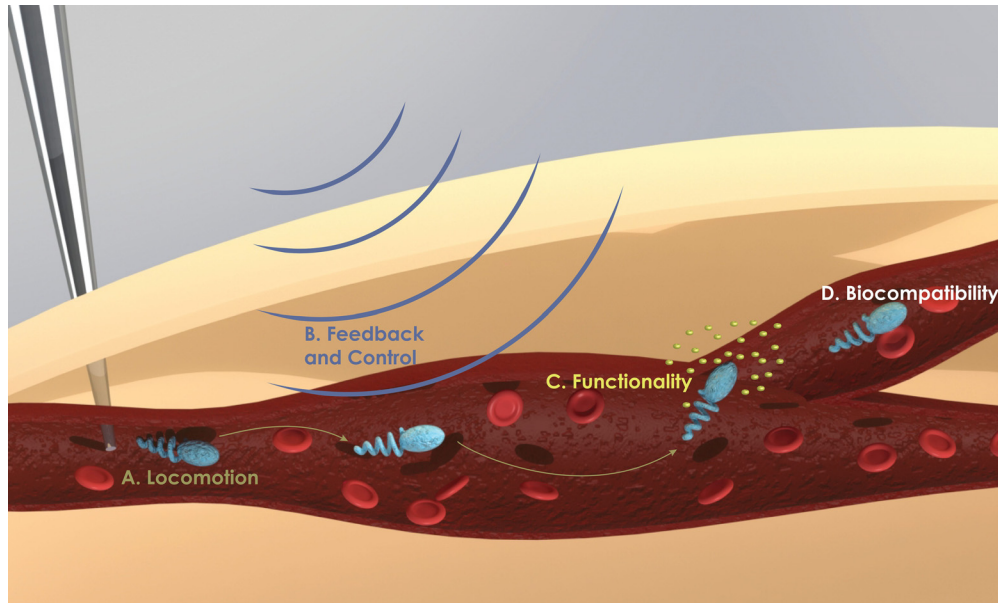


FIG. 1. Design elements of a medical microrobot (MMR). An ideal MMR for implanted medical application must have (1) a method for moving from a given environment with minimal damage to surrounding features, whether it is fluid, soft tissue, or a boundary location; (2) responsiveness, so that it can adapt to real-time conditions, either by intrinsic controls based on physiological sensing or by extracorporeal control modalities, such as ultrasound or magnetism; (3) a sensing or intervention-oriented medical functionality, such as a drug or cell delivery; and (4) sufficient biocompatibility of materials to minimize any immune response and thereby maximize the life span of the device *in vivo*.

movement of the MMR and movement of device features within the MMR.

1. Within a liquid

The circulatory system is the highway of the body and thus a logical location for MMRs to maneuver, either with or against blood flow. The most basic devices for maneuvering through fluid systems are synthetic devices of simple geometric shapes, typically a bead or a cylinder. For a simple case of a microsphere moving through a Newtonian liquid, the forces can be expressed as those exerted by the device upon the surroundings and those exerted by the surroundings upon the device

$$\mathbf{F}_G + \mathbf{F}_B + \mathbf{F}_d = 0, \quad (4)$$

where the difference between the gravitational force \mathbf{F}_G and the buoyancy force \mathbf{F}_B determines the acceleration of the microsphere; the device reaches a steady velocity when the \mathbf{F}_d increases as a response to the increasing velocity such that the forces cancel each other out, with the viscous drag force for a sphere at low Reynolds number

$$\mathbf{F}_d = 6\pi\mu R\mathbf{u}, \quad (5)$$

where the viscous drag force is dependent on the sphere's radius R , the dynamic viscosity of the fluid μ , and the fluid velocity \mathbf{u} .⁴⁵ Indeed, in one of the first *in vivo* demonstrations of an MMR, Martel *et al.* applied these principles for a small sphere in blood to magnetically actuate a 1.5 mm ferromagnetic bead through the carotid artery of a porcine model.⁴⁶ The effects from gravitational weight and from buoyancy can be simplified into an apparent weight force, \mathbf{F}_{AW} [Fig. 2(b)].⁴⁷

However, blood is a non-Newtonian fluid, in that its viscosity depends on how much stress is placed on it and is classified as a “shear-thinning” liquid, becoming less viscous with increasing shear stress. In blood vessels, this manifests as a decrease in viscosity in large blood vessels as blood flow speed increases, as shearing causes red blood cell chains to break into shorter and shorter chains.⁴⁸ In contrast, viscosity increases in extremely small blood vessels, particularly in capillaries that have a smaller effective diameter than some red blood cells.⁴⁸ Therefore, the hemodynamics are dramatically different in large and small vessels, and microrobots should be designed with conditions of the intended vessels considered carefully. Relatedly, as shown in Table I, the geometry of a bead is suited for the conditions of a large vessel, but ineffective in smaller passages, whereas MMRs consisting effectively of a bead with a tail are more suited for smaller vessels. This is best understood by considering that the locomotion of an MMR occurs when the ratio of an applied motive force \mathbf{F}_m on the MMR is maximized relative to the total force experienced by the MMR. While the motive force for a bead corresponds to r^3 , the motive force for a bead with tail corresponds to r^2 .⁴⁹ Furthermore, the drag force \mathbf{F}_d on the MMR relates to r^2 in a large vessel and to r in a small vessel; \mathbf{F}_d is also dependent upon the amount of vessel occlusion that occurs.⁴⁹ Scalar factors are additionally significant for considering MMRs with magnetically pulled locomotion, as drag forces decrease linearly with characteristic dimension at low Reynolds numbers, while magnetic forces scale down at cubic rates.⁴⁹

For more complex passageways, such as bifurcations or partially obstructed vessels, microrobots must have adaptable designs, often-times mimicking the techniques of microswimmers in nature. As previously introduced, since propulsive force is balanced by viscous (Stokes) drag forces, microorganisms rely on periodic but not

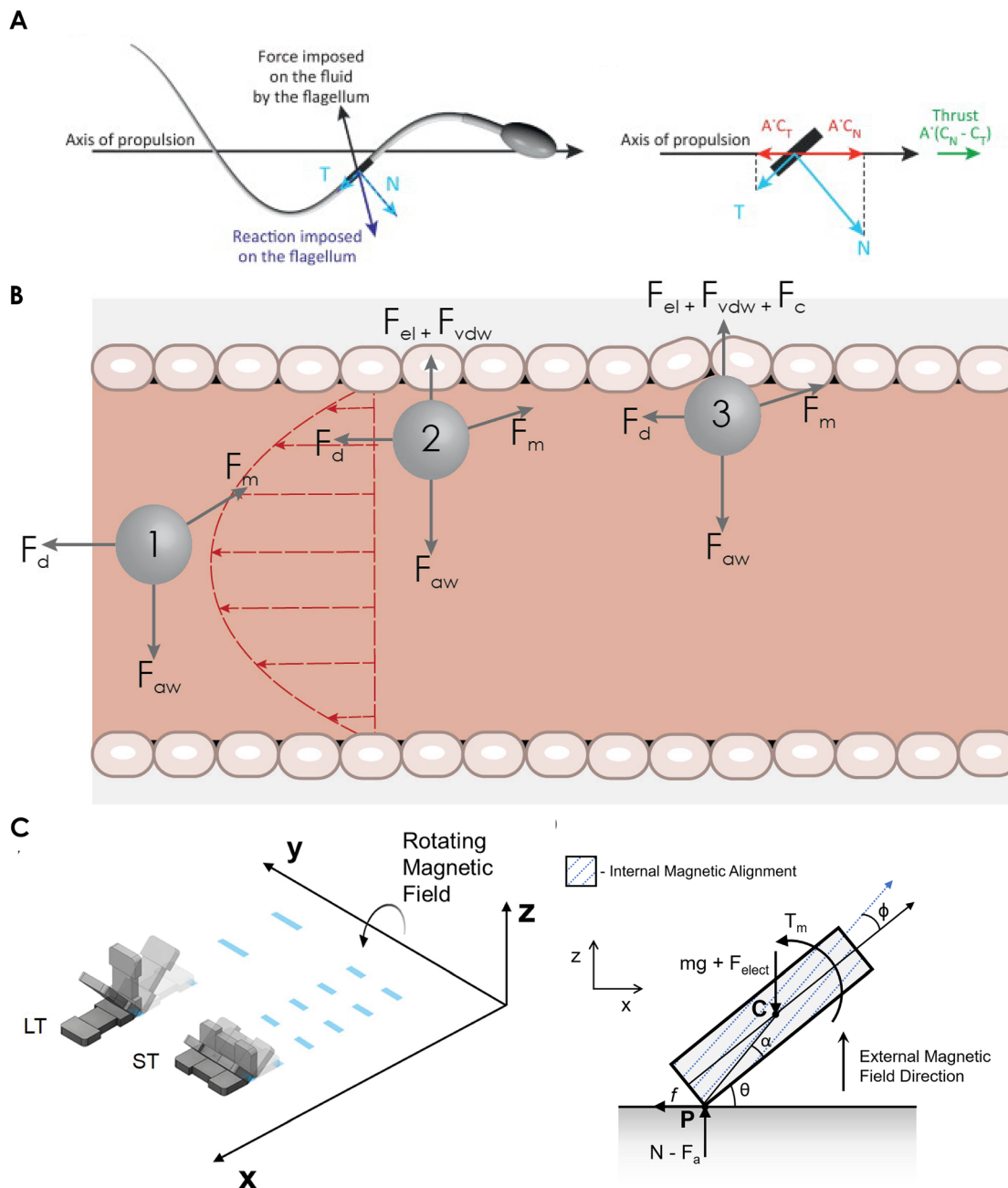


FIG. 2. Locomotion considerations for different environments in the human body. (a) Left: Diagram of a sperm cell, a common biological model of a microswimmer designed for low Reynolds number environments, pushing through the fluid. The force of the sperm tail against the fluid (black) induces a reaction force from the fluid against the tail (dark blue, with tangential (T) and normal (N) force vector components in light blue). Right: The tangential drag coefficient (C_T) and normal drag coefficient (C_N) correlate with the corresponding force vector according to a proportionality factor (A); the larger value of C_N , relative to C_T , causes anisotropic friction and thereby facilitates the microswimmer's movement forward.²⁰⁵ Reprinted with permission from Alvarez *et al.*, Trends Cell Biol. **24**, 198–207 (2014). Copyright 2014 Elsevier. (b) The most relevant forces acting upon an MMR vary, as demonstrated by an MMR with a motive force oriented toward a point in the vessel wall, which passes through the center of the vessel,¹ steers closer to the vessel wall,² and comes into contact with the bordering endothelial cells.³ The forces shown are the most relevant forces for each environment, but not an exhaustive diagram of the forces acting upon the MMR. (c) Left: A demonstration of a microrobot that tumbles across a solid surface, either in a lengthwise tumble (LT) or sideways tumble (ST), depending on the alignment of embedded magnetic particles. Right: In this case, the relevant forces with respect to the motion of the microrobot are electrostatic force F_{elect} , adhesive force F_a , normal force N , and magnetic torque T_m . Other relevant parameters include the center of mass C , contact point P , alignment offset angle ϕ , angle between the corner of the robot and its center of mass α , and the orientation angle θ .⁷⁰ Reprinted with permission from Bi *et al.*, Micromachines **9**, 68 (2017). Copyright 2017 Author(s), licensed under CC BY.

TABLE I. Locomotion in blood vessels. The dominant relevant forces on a micromachine varies, depending on both the environment and the properties of the microrobot. Notably, different MMR geometries are better suited to certain environments, as indicated by the ratio of the MMR's motive force relative to the total forces acting on the MMR.⁴³ In this comparison of MMR locomotion in the blood stream, “+++” represents when it is likely that $F_m/F_{total} > 1$ (indicating that it will be able to move more successfully against blood flow), “++” represents when F_m/F_{total} may fluctuate between <1 and >1 , and “+” represents when it is likely that $F_m/F_{total} < 1$. This assumes an equally total volume for all compared geometries and a certain amount of geometry optimization. Furthermore, the optimization of such force dynamics can vary greatly based on biological parameters.

Application site	Sphere	With helical tail	With beating flagella tail
Large vessel	+++	+	+
Medium vessel	++	++	++
Small vessel	+	+++	+++

reciprocal motion to achieve propulsion. For instance, cilia achieve thrust by performing an effective stroke which experiences high drag by moving perpendicular to its central node, and a recovery stroke that induces low drag by moving in parallel, while bacteria flagellum uses propellerlike motion (which converts rotary motion to forward or backward thrust) to move through a respective microenvironment.^{50–54} These two methods of movement are most, respectively, appropriate for different environments, where planar flagellum is best suited to low-viscosity environments, and helical tailed-devices high-viscosity environments (Table I).⁵⁵ de Lima Bernardo and Moraes demonstrated an integrated model for the dynamics of a helical flagellum that determined an optimized geometry when the helical tail makes a 35.3° angle with the axis of the device's head.⁵⁶ There have been numerous microrobotic systems demonstrated, both *in vitro* and *in vivo*, that have employed bacteria-inspired techniques for movement through liquids.^{57,58} An MMR with a planar tail and tubular body operates best in low viscosity and in situations of vessel endothelium penetration,^{55,59} while an MMR with helical tail functions ideally in high-viscosity environments.^{55,60} Soft-hydrogel MMRs with strategically embedded magnetic nanoparticles (NPs) can adapt to complex environments with varying viscosities by applying origami folding principles to selectively change body geometry, such as by transitioning between a “stumpy” and “long slender” form depending on surrounding conditions.^{55,59}

As microrobots maneuver through increasingly restricted vessels, the effect of surface forces, primarily Van der Waals, electrostatic, and capillary forces becomes more significant in determining whether these devices can effectively move. These forces will be considered in more depth within Subsection II A 2.

2. At tissue boundaries

Separate from migration within the blood vessels, it may be important for some MMRs to either dock on a vessel wall or migrate from the transport conduit of the bloodstream into a desired tissue region. The boundary between blood and solid tissue presents unique force conditions and demands further specialized movement techniques.

Similar to microswimmers in fluid, nature can inspire boundary movement techniques, namely, amoeboid-style crawling or leukocyte-

based rolling movement.^{61,62} The simplest model for considering such surface movement is to consider a spherical microrobot being pushed or pulled by an external propulsive force along some surface, through either liquid or air. In the case of pulling- or pushing-based surface movement, sliding would occur when the externally applied motive force F_m overcomes sliding static friction F_s , while steady-state velocity occurs when the $F_m = F_k$, the kinetic sliding friction force.⁶ The energetic cost of transport for this type of movement depends upon velocity v , stride length λ_s , viscous drag coefficient b , kinetic friction coefficient μ_k , and body mass m .⁶ This model demonstrates that high speeds and small steps are energetically costly for MMRs that move via external pulling or pushing, or via crawling; such MMRs move most effectively when the body shape and size are optimized to minimize b , the viscous drag coefficient, due to the large energetic penalties associated with a large drag coefficient. Relatively, MMRs that employ rolling-based motion along surfaces have much lower energetic obstacles, since the motive force needs only overcome apparent mass and rotational friction, a much lower friction than that of sliding friction.⁶³ Such considerations for movement along surfaces with minimal resistance are particularly relevant for devices moving in the bloodstream, when the MMRs may come into close contact with vessel walls.⁴⁹

As previously mentioned, these devices also experience surface forces, including Van der Waals and electrostatic forces, as well as contact forces. The prominent surface forces between a microrobot of radius R and flat surface (S) are⁶⁴

$$F_{vdw} = -\frac{A_{MR-S}R}{6D^2}; \quad F_{el} = \frac{q\sigma}{2\epsilon_0\epsilon}. \quad (6)$$

The Van der Waals force, F_{vdw} , depends on the distance D between the microrobot and surface, the microrobot radius R , and the Hamaker constant of the interaction A_{MR-S} , which is determined based on each element's respective Hamaker constant $A_{MR-S} = \sqrt{A_{MR}A_S}$.⁶⁴ The electrostatic force, F_{el} , is the force applied by the surface charge density σ of the surface on the electric charged particle q of the microrobot, which is determined based on the relative dielectric constants of the medium and a vacuum.⁶⁴ Both of these forces are relevant whenever a device is within a relevant range of the solid surface. The contact force differs between instances of adhesion and pull-off; the most suitable model for this force depends upon the velocity of the device.^{49,64,65} The effects of surface forces such as Van der Waals or electrostatic forces can also have an impact on MMRs within the bloodstream; these forces can counterbalance drag force effects when close to upper vessel walls, while enhancing drag near vessel walls.⁴⁹ There are additional forces that may apply, dependent on conditions, such as the steric interaction force between a microrobot's polymeric chains and a vessel wall's glycocalyx, hydrophobic forces, and double-layer forces.^{49,64,66} Furthermore, MMRs composed of soft materials, when colliding with a surface at a tissue boundary or under load, could experience large shape deformation and, over time, volume deformation.^{67–69}

Consideration of these additional environmental forces has spurred a variety of innovative device geometries and morphologies for surface movement, to both minimize effective volume or surface area and improve the likelihood of biocompatibility (Table I). For instance, a rigid device fabricated in a dumb-bell structure, with the ends oppositely magnetically charged, can be activated with an

alternating magnetic field to have a tumbling movement mechanism, with both lengthwise and sideways tumbling possible depending on the orientation of embedded magnetic particles [Fig. 2(c)].⁷⁰ These microdevices successfully navigate movement in both wet and dry environments, including up incline planes. The devices move more slowly but precisely in high-drag environments; they require less propulsive force in high-density environments because of improved buoyancy, albeit with increased slippage because of reduced friction force. In dry environments, drag and buoyancy are minimal, and so high tumbling speeds were observed. In contrast to these rigid devices, flexible and small-scaled silicon elastomer devices with embedded magnetic NPs, which are programmed to have a single-wavelength harmonic magnetization profile along the length of the body, have been shown to have a diverse ability of gymnasticlike properties, ranging from meniscus climbing at a surface between water and air, to jumping when in solely air.³⁴ Although this device has thus far only been demonstrated *in vitro*, its potential medical applications are wide-ranging.

3. In swarms

In addition to environmental forces, a micromachine can also be affected by the proximity to other similarly scaled devices; many of the forces that apply between a microrobot and a wall surface would similarly apply between two microrobots, such as contact, Van der Waals, electrostatic, and steric forces. For instance, the Van der Waals forces between two microrobots, each consisting of a simple microsphere, is modeled as

$$F_{vdw} = \frac{A}{6D^2} \frac{R_1 R_2}{(R_1 + R_2)}, \quad (7)$$

with respective device radii R_1 and R_2 , the distance of separation D , and A as the Hamaker constant.^{71,72} Microrobots intended for swarm applications must produce sufficient motive forces to overcome these additional surface and contact forces which may hinder movement.^{2,73,74}

4. Summary

Overall, the general force balance equation to consider for an MMR is

$$\frac{dv}{dt} = F_m + F_d + F_{AW} + F_{vdw} + F_{el} + F_c, \quad (8)$$

which considers the relevant of contact force F_c , motive force F_m , hydrodynamic drag force F_d , apparent weight F_{AW} , Van der Waals force F_{vdw} , and electrostatic force F_{el} [Fig. 2(b)].^{6,49,75,76} This general equation must be adjusted depending on specific conditions of the device and the system, such as interaction with boundary walls or other MMRs.

B. Feedback and control

MMRs must be responsive and adaptive once introduced into the human body; therefore, these devices must be controllable via a variety of possible modalities. Previous works have noted a need for wireless signals for the purpose of localization and tracking of the MMR.⁴ In recent years, autonomous robots with well-developed control

systems^{77,78}—from autonomous mobile robots in warehouses to unmanned aerial vehicles—have demonstrated a fundamental need for bidirectional signals (e.g., sensing information from robot to a controller and functional signals from controller back to robot), with a robust method for signal processing in the controller (which could include machine-learning approaches). This paradigm of a feedback and control system,⁷⁹ as applied for MMRs, is shown in Fig. 3. Three different schemes are possible: A manually controlled extracorporeal control system, an automated extracorporeal control system, and an automated internal control system. A primary consideration is the location of the controller, the element that processes signals from sensors and sends instructions for locomotion or functionality back to the MMR. The controller can be either extracorporeal (outside the human body) or intrinsic (embedded within the MMR). Most approaches for MMRs rely on extracorporeal controllers as they are less constrained by space and power. Extracorporeal control is also versatile, allowing for manual intervention, as well as machine-learning algorithms for closed-loop operation (i.e., automation of the function of the MMR without manual intervention). On the other hand, MMRs with an intrinsic controller—functionally similar to a cell, micro-organism, or organ—could be compact and autonomous. However, it is currently challenging to engineer MMRs with intrinsic control mechanisms beyond simple stimuli-responsive materials (possible approaches to engineer control mechanisms with complex logic include molecular machines⁹ and synthetic biology⁸⁰). Intrinsically controlled MMRs would also fall outside of mechanisms for manual intervention should it be required.

Common control modalities include magnetic, ultrasound, thermal, and optical mechanisms (Table II). While alternative control methods have been proposed such as electric, near-field control, and radio frequency, these techniques often require the incorporation of more traditional MEMS components, and thus we have chosen to exclude such devices from the scope of this review, despite their interesting possibilities (for example, as injectable sensors).^{81–83} When considering the appropriate control modality for a certain application, it is important to consider the needed range, depth of penetration, and resolution, as well as the capital equipment required. Furthermore, feedback and control mechanisms are crucial in minimizing any associated risks pertaining to MMRs, particularly by reducing the likelihood of damage to the surrounding tissue.

1. Extracorporeal controller

a. Magnetic modality. Magnetically controlled MMRs can operate in a wide-ranging depth of field; most demonstrations of this technology focus on methods for manipulating devices through fluid-filled areas of the body, such as blood vessels or the eye.⁴ These early demonstrations have garnered interest as a method to deliver drugs to locations within the body which are otherwise challenging to target precisely (e.g., remote blood vessels) or to perform wireless surgery in regions near a fragile tissue (e.g., the retina) (Table II).^{101,102}

MMRs can achieve magnetic control either by being coated with magnetic materials such as nickel or by embedding magnetic NPs within their structure, allowing for responsiveness to external magnetic or electromagnetic devices, with the extent of responsiveness dependent upon the type of the magnetic material used, namely, ferromagnetic or paramagnetic materials. Ferromagnetic materials on the

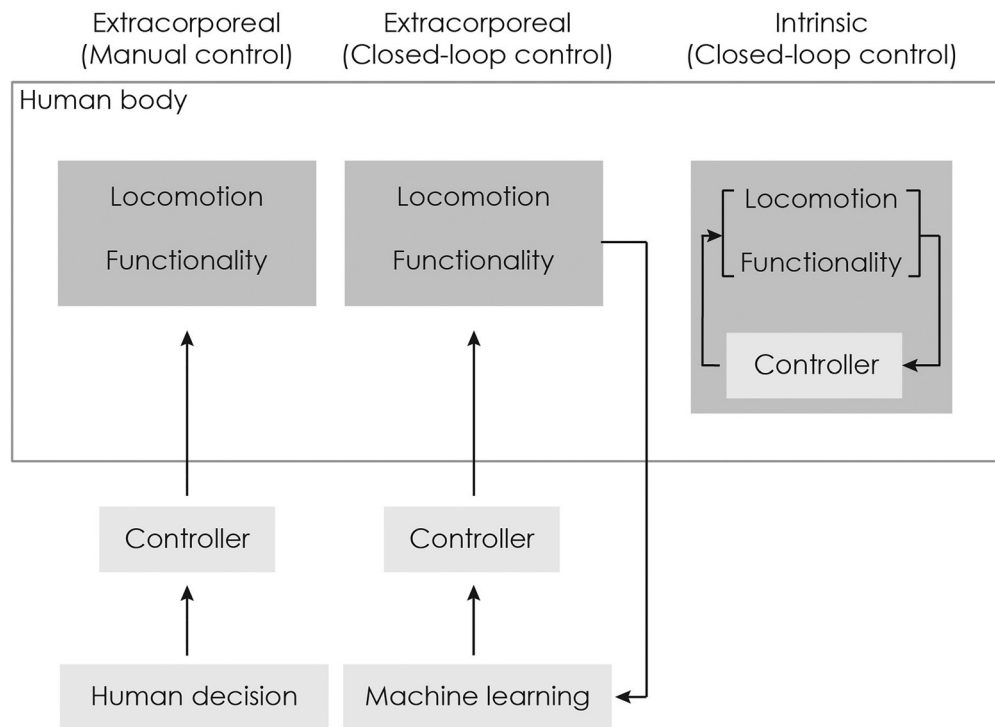


FIG. 3. Mechanisms for feedback and control of an MMR. Three schemes are shown, with two involving a controller located outside the human body which can wirelessly receive and send signals to the MMR, and a third where the control mechanism is embedded within the MMR itself. A manual control mechanism allows for manual intervention and control, whereas an automated control mechanism (either one using machine-learning or one with an intrinsic controller) allows for an autonomous operation. Note that the darker gray box represents the MMR.

macroscale, such as iron or nickel, maintain their magnetic properties even after a magnetic field is removed, whereas paramagnetic materials such as platinum and aluminum are only magnetic upon exposure to magnetic fields. Palagi *et al.* demonstrated that micromachines embedded with paramagnetic particles were magnetically propelled, while those embedded with ferromagnetic particles were both propelled and reoriented with respect to the magnetic field.¹⁰³ However, a ferromagnetic material on the scale of nanometer-sized particles exhibits the same lack of hysteresis as a paramagnetic material and the higher magnetic susceptibility of ferromagnetic materials; such particles are considered superparamagnetic. Superparamagnetic MMRs differ from other magnetic methods because these devices do not exhibit remnant magnetization when not exposed to the magnetic field, are easier to fabricate, experience relatively less toxicity challenges, and do not undergo agglomeration of adjacent MMRs in the absence of an applied magnetic field.¹⁰⁴ Morozov *et al.* fabricated superparamagnetic MMRs and showed the propulsive capacities of these devices as correlating to “steerability” based on device geometry and to the material’s magnetic susceptibility.¹⁰⁵ The ability to orient the devices can be useful for certain tasks, particularly the ones that require precise movements. Furthermore, the speed of the devices can be controlled by the density of embedded charged NPs; although current demonstrations have only achieved speeds an order of magnitude slower than the speeds of cerebrospinal fluid, there remain many opportunities for the optimization and improvement of speed.

External magnetic sources, which vary in terms of equipment, can control the translational and rotational movements of magnetic MMRs, by generating an external magnetic field, with magnetic flux density \mathbf{B} , which magnetizes MMRs, and causes them to experience a magnetic torque, τ , and force, \mathbf{F}

$$\tau = V\mathbf{M} \times \mathbf{B}, \quad (9)$$

$$\mathbf{F} = V(\mathbf{M} \cdot \nabla)\mathbf{B}, \quad (10)$$

where \mathbf{M} is the magnetization of the object, V is the volume of the magnetized object, and where $\nabla\mathbf{B}$ points toward the direction of the highest flux density. These expressions demonstrate that a magnetized MMR will move toward “a local maximum of the field” due to the magnetic force and that a magnetic MMR will rotate due to torque, because torque causes the device to align with the magnetic field, and as such, a rotating magnetic field will cause the device to rotate.⁶²

Permanent magnets can be used to communicate with subcutaneous MMRs. In our own work, Chin *et al.* developed an implantable hydrogel-based microdevice with locking gears and separated chambers with superparamagnetic iron oxide NPs for controlled and dosage-related drug delivery.³⁸ We demonstrated that the ability applies to a permanent magnet approximately 1 cm from the device surface to rotate a gear within the device, in order to facilitate drug release from a selected chamber of the device.³⁸

For applications seeking a more diverse range of motion or a greater depth of penetration, the application of electromagnetic coils

TABLE II. Feedback and control modalities. Comparison of key characteristics for the most common control modalities and mechanisms for MMRs.

Modality	Magnetic	Ultrasound	Near-infrared (via photothermal effect)
Depth of penetration	>100 mm ⁸⁴	100 mm ⁸⁵	Up to 100 mm, dependent on tissue type ⁸⁶
Resolution ($x \times y$)	1 × 1 mm is standard at 3 T from MRI machine, for depths of 30–100 mm ⁸⁷	Depends on the depth of penetration, e.g., 40 × 40 μm at a depth of 2.5 mm ⁸⁸	Depends on the depth of penetration, e.g., for thicknesses > 1 cm, resolution is 1/5 of thickness ⁸⁹
Risk of tissue damage	Heavy metals (e.g., Pt, Au, Ni, Co, and Ag) may be harmful to living cells and tissues ⁹⁰	Potential tissue deformation and damage; ⁹¹ heavy metals may be harmful to living cells and tissues ⁹⁰	Risk for tissue damage due to resulting hyperthermia ⁹²
Capital equipment	Permanent magnet, electro-magnet system, or MRI machine ^{38,93,94}	Ultrasound transducer	NIR light integrated laser system
Responsive materials	Magnetic, e.g., Ni, Co, or Fe coating, nanowires, or NPs ⁹⁰	Asymmetric geometry, to enable acoustophoresis; ^{95,96} thermoresponsive materials ⁹⁷	Thermoresponsive material embedded with NIR-sensitive nanomaterials, e.g., gold or carbon nanomaterials ⁹²
Limitations	Lack of biodegradability of magnetic NPs; potential toxicities due to high concentration of magnetic NPs in the localized area; risks associated with very high-powered MRI machines ⁹⁸	Maximum speeds can be too low to overcome blood flows; ⁵⁸ some US-controlled MMRs require fuel for locomotion ⁹⁹	Limited demonstrations of biocompatibility and biodegradability of NIR-sensitive nanomaterials; ¹⁰⁰ poor resolution ⁸⁹

may be appropriate (Table II). Martel *et al.* first demonstrated the adaptation of a conventional MRI system for propelling and navigating a 1.5 mm ferromagnetic bead through larger blood vessels in a porcine model.⁴⁶ Felfoul *et al.* improved upon this technology by introducing a method for simultaneously imaging and propelling an implanted magnetic millimeter-scale device, which exhibited 95% of the force generated by prior systems while imaging at 27 Hz.¹⁰⁶

Kummer *et al.* developed a customized device, containing several soft-magnetic-core electromagnetics, which can produce nonuniform magnetic fields, in contrast to the uniform magnetic fields and gradients produced by the orthogonal electromagnets of an MRI machine.⁹³ This asymmetry facilitates a 5-degree of freedom (DOF) control of implanted MMRs, with a 2-DOF pointing orientation and a 3-DOF position; the MMR has an unrestricted rotational DOF. Diller *et al.* designed a technology that improves control flexibility by allowing 6-DOF, facilitating the ability to apply magnetic torque about the magnet's magnetization axis and thereby allowing maximal flexibility of orientation.¹⁰⁷

Thus far, most demonstrations of magnetically controlled MMRs have emphasized either guiding or guiding and propulsion of biologically inspired microswimmers, with both flexible tail and helical geometry; several research groups have demonstrated successful *in vivo* demonstrations for ocular and cardiac applications.^{4,46} Given the deep range of tissue penetration and increasingly improving resolution capabilities (Table II), magnetically controlled MMRs have the potential for applications throughout the body.

b. Ultrasound modality. Although traditionally an imaging modality, ultrasound functions as a control modality that can propel both catalytic and fuel-free devices, as well as facilitate external steering; prior demonstrations employ both direct ultrasound-generated radiation force and control via ultrasound-generated heat or cavitation bubbles.¹⁰⁸ Ultrasound provides numerous advantages and opportunities, namely, low cost, minimal health risks, and quick and high imaging resolution.⁴ Generally, ultrasound-controlled microrobots can swim by locally converting resonating ultrasound into spinning and directional motion, with the ability to move quickly, up to 200 μm/s.⁵⁸ Ultrasound localization applications exhibit 150–200 mm penetration depths and a 500 μm resolution, with limitations pertaining to bone and air bubbles (Table II).¹⁰⁹

While surface acoustic waves can noninvasively accomplish numerous important skills for lab-on-a-chip systems, such as cell-cell interactions, separation circulating tumor cells, and patterning microparticles, much of the development in controlling and propelling micromotors relies upon ultrasonic standing waves, namely, continuously applied continuous waveforms with fixed frequency and a voltage determined according to the needed intensity of the ultrasonic wave. As Nadal and Lauga demonstrated, a given microsphere oscillating in a fluid can be propelled along the particle's axis of symmetry and perpendicular to oscillation direction by steady streaming in a fluid, which exert steady stress upon a particle.^{95,110}

The application of an active transducer against a reflector can result in the development of an ultrasound standing wave field,

characterized by nodes of maximal pressure and of zero pressure. This pressure has a primary radiation force experienced by individual particles, which causes particle migration or collection in a pressure node area, and a secondary radiation force experienced between particles, which causes the particles to repel or attract each other.¹¹¹ This primary radiation force is defined as

$$F_{rad} = \left(\frac{-\pi P_o^2 V \beta_o}{2\lambda} \right) * \phi * \sin\left(\frac{4\pi z}{\lambda}\right), \quad (11)$$

with ultrasound standing wave field (USWF) peak pressure amplitude P_o , spherical particle volume V , field wavelength λ , perpendicular distance on axis from pressure nodal planes z , and acoustic contrast factor ϕ ,

$$\phi = \frac{5\rho_p - 2\rho_o}{2\rho_p + \rho_o} - \frac{\beta_p}{\beta_o}, \quad (12)$$

which is determined by particle compressibility and density ρ_p and β_p , respectively, and the surrounding medium compressibility and density ρ_o and β_o .¹¹² Generally, the primary radiation force determines particle distribution for ultrasound-based particle manipulation and enables particle patterning based on the controlled application of ultrasound standing waves, with a particle held at each primary force minimum when the wavelength is close to the particle size.¹¹³

Some of the first demonstrations of ultrasound-controlled microrobots were nanorods that employed ultrasound for assist in various catalytic reactions to enable propulsion. This method facilitates high-speed movement through areas of high viscosity, such as dense organs and tissue, more in a more energetically efficient and precise manner than solely magnetic-based methods.¹¹⁴ For instance, Xu *et al.* fabricated poly(3,4-ethylenedioxythiophene) (PEDOT)/Ni/Pt microrods that rely on catalytic reactions to eject bubbles; ultrasound-dependent microrods respond more quickly than optical- and heat-based control systems due to primary radiation force.¹¹⁵ A similar technique utilized ultrasound to vaporize bound perfluorocarbon emulsions from the interior surface of the MMR, for bubble-fueled propulsion.¹¹⁴ Such ultrasound-powered micro- and nanorods are capable of a flexible motility, rapid responsivity, delivering large payloads, and having a wide range of functionalization systems. They can aid in drug delivery, cell patterning, and cell control and propulsion.

More recent ultrasound-based control demonstrations have emphasized the opportunities for a fuel-free and biocompatible external control mechanism, by using the ultrasound wave as a direct impetus for propulsion.⁹⁵ Wang *et al.* demonstrated, in that ultrasonic standing waves in the MHz frequency range can manipulate metallic microrods in water in a variety of manners, including for propulsion and orientation.⁹⁵ This group's more recent work demonstrated a more precise axial movement dependent upon shape asymmetry for bimetallic nanorods and a correlation between longer rod lengths and decreased maximum speed.¹¹⁶ Garcia-Gradilla *et al.* demonstrated potential utilities for these ultrasound-dependent nanorods by functionalizing Au-Ni-Au nanorods with relevant antibodies to capture and transport cells.⁹⁶ Although the mechanism for acoustic propulsion is not entirely understood, a hypothesis is that interference between standing acoustic waves creates a differential pressure field. The primary radiation force balances the microrobot at the minimum-pressure plane, which the rod-shaped microrobot assembles into a longer spinning chain assembly due to secondary radiation forces;

asymmetry in a nanorod's shape, such as a concave distal end, translates into a random motion at the balancing plane.^{90,116,117}

While most ultrasound-controlled microrobots and MMRs are made of hard materials such as metals, there are emerging applications of ultrasound-responsive hydrogels in nonlocomotive micromachines. For example, hydrogels have been shown to be responsive to ultrasound either by triggering changes in the crosslinking¹¹⁸ or, in our work, by incorporating thermally responsive polymers.⁹⁷

c. Near-infrared (NIR) modality. The therapeutic window of near-infrared (NIR) light (650–1100 nm¹¹⁹) is an increasingly popular method of external stimulation due to its deep tissue penetration, minimum scattering, reduced phototoxicity, relatively low-cost equipment, and accurate spatiotemporal control.¹²⁰ Unlike high photon energy UV or visible (UV-vis) light which have a limited depth of penetration due to high absorbance by hemoglobin, NIR can penetrate up to 10 cm into breast tissue and 4 cm into muscle tissue when using microwatt laser sources.⁸⁶ NIR has been used in a number of clinical applications, such as monitoring blood oxygenation levels, for imaging purposes, and photothermal cancer therapy. Implantable or injectable NIR-responsive systems are usually controlled by one of the following mechanisms: Photothermal effect or upconversion (two-photon absorption, upconverting NPs).

The photothermal effect harnesses NIR irradiation by converting applied NIR energy to heat, which is then dissipated into the surrounding environment to raise the local temperature. Microrobots, which are responsive to NIR via the photothermal effect, are typically composed of a thermoresponsive material embedded with NIR-sensitive nanomaterials (i.e., gold NPs, carbon nanotubes, iron oxide, or graphene oxide), such that the conversion of NIR light into heat by the nanomaterials triggers a physical process such as swelling/deswelling or sol-gel transition of the thermoresponsive material. The use of NIR-sensitive nanomaterials composed of noble metals can enhance light absorption via localized surface plasmon resonance, where the electric field of the incident light drives the collective oscillation of free electrons,¹²¹ which can then be converted to heat. The majority of NIR-responsive microrobots (MRs) are stimulated via the photothermal effect, to enable shape changes in the thermoresponsive material, for optimal locomotion⁵⁹ or drug delivery.^{122–124} However, limitations associated with this mechanism include potential cytotoxicity from the resulting hyperthermia, as well as complications due to the lack of biocompatibility and biodegradability of many NIR-sensitive nanomaterials⁹² (Table II).

Many light-sensitive drug-delivery systems involving photo-initiated reactions, such as isomerization or bond cleavage, are responsive to higher photon energy UV or visible light, rather than lower energy NIR irradiation. However, the clinical translation of UV-vis-responsive systems is limited due to their phototoxicity and limited depth of penetration. The process of upconversion takes advantage of the higher energy of UV-vis light (in comparison to NIR) along with the deeper penetration of NIR light (in comparison to UV-vis) by essentially converting NIR light into UV-vis light, to enable the use of UV-vis-responsive systems with NIR irradiation. One form of upconversion is two-photon absorption: chemical groups sensitive to UV-vis irradiation simultaneously (within femtoseconds) absorb two NIR photons to achieve higher energy excited states, similar to absorbing one photon of UV-vis light.^{120,125} However, two photon absorption

has low excitation efficiency, which is proportional to the square of the intensity of the incident light, thereby requiring the use of pulsed lasers with high power densities; such lasers are expensive and have a small field of view, limiting their clinical use.^{125,126} Another form of upconversion uses upconverting NPs, typically lanthanide-based NPs, that can sequentially absorb two NIR photons and then re-emit one higher energy photon in the UV-vis range.¹²⁰ Limitations of this mechanism involve the unknown biocompatibility, low quantum yield, and rapid heating effects because the excitation wavelength of many upconverting NPs overlaps with the absorption peak of water.¹²⁷

2. Intrinsic controller

As well as being controlled by the aforementioned external modalities, MMRs can also be controlled via an intrinsic mechanism that directs the MMR to perform a particular functionality when the device senses a particular environmental stimulus. Biohybrid MMRs often capitalize on their incorporated cellular component as a sensor, to enable a taxis response to an environmental stimulus.^{29,57} The pH-taxis of *Serratia marcescens*¹²⁸ and aerotaxis of the *Magnetococcus marinus* strain MC-1¹²⁹ have been leveraged to design biohybrid MMRs to target tumors which are typically hypoxic and have low pH levels, respectively. Biohybrid MMRs can transport cargo to a specified location by taking advantage of the ability of cells to sense their environment and autonomously move toward or away from a particular stimulus, where they can perform a functionality such as cargo release. Conversely, in hydrogel-based micromachines, the hydrogel can act as the sensor, by swelling/deswelling upon sensing an environmental stimulus such as pH.¹³⁰ In the future, directions can include the incorporation of on-board electronics, but such approaches will need to address powering (requiring solutions such as fuel cells¹³¹ or wireless charging) and biocompatibility.

C. Functionality

Upon reaching a target location, MMRs carry out a function in response to an extracorporeal or intrinsic trigger. Here, we will discuss

specific requirements for MMRs depending on their intended functionality, such as sensing particular analytes in the surrounding environment, triggered delivery of small molecules or larger cargo such as cells, or microgripping to a tissue for surgical excision (Table III).

1. Sensing

MMRs capable of sensing analytes and providing a readout to the patient or medical professional usually have two components: a receptor that specifically binds or recognizes the target analyte and a transducer that converts the biorecognition event into a signal that can be read out by the user.¹⁴⁷ Currently, the majority of sensing MMRs are not composed of soft materials and have mostly been developed for *in vitro* applications.¹⁴⁸ Mechanisms commonly used by these types of devices include motion-based chemical sensing that translates changes in the concentration of an analyte into specific MMR mechanical motions that can be optically read out; electrochemical sensing that produces an electrical signal from a reaction with the analyte of interest, and fluorescence or luminescence sensing¹³⁶ that can indicate analyte concentration from fluorescence, luminescence, or colorimetric levels. These mechanisms could potentially be applied to devices for *in vivo* applications; for example, although not composed of soft materials, Ergeneman *et al.* incorporated luminescence sensing into a minimally invasive, magnetically controlled intraocular oxygen sensor.^{132,133} Microrobots can also function as force sensors, by deforming a microfabricated beam, cantilever, or spring with a known stiffness to measure the applied force. For example, Kawahara *et al.* developed magnetically controlled microrobots, in which an externally placed magnet can actuate a beam in order to apply a force to single cells, which can then be estimated based on the degree of beam deformation.¹³⁵ Though the majority of force sensing microrobots have been developed for *in vitro* applications (in tissue culture plates or microfluidic devices),^{134,135} modified designs that miniaturize the microelectronics may be useful for MMRs to differentiate between healthy and abnormal cells based on mechanical properties^{2,149} or for targeted tissue excision or targeted therapies. In the future,

TABLE III. Functionality. Description of commonly desired functions of an MMR. Depending on the intended functionality, the key parameters of a microrobot vary significantly.

	Important considerations	Examples
Sensing	Incorporation of receptor (to bind target analyte) and transducer (to convert the bio-recognition event into a signal that can be read out)	References 132–136
Delivery of drugs and small molecules	Sufficient drug loading (e.g., via encapsulation within hydrogel mesh or compartmentalization within a device) <i>In vivo</i> drug stability	References 97, 122–124, 130, and 137–139
Delivery of cells	Sufficient cell loading (e.g., via encapsulation within a porous hydrogel or compartmentalization within a device) Maintenance of cell viability	References 17, 23, 123, 138, 140, and 141
Gripping	Mechanical robustness to ensure that the device does not deform or fracture while gripping the target	References 142–146

biocompatible electrodes for neural recording (and electrical stimulation)^{150,151} could be an additional element for MMRs.

2. Delivery of drugs and small molecules

Drug delivery is a key functionality for soft MMRs, as they can load substantial amounts of drugs and small molecules and they can be triggered to release the drug on demand. Unlike microrobots composed of hard, rigid materials, which have limited cargo loading on their surface, hydrogel-based devices can increase drug loading by encapsulating drugs within their mesh. Furthermore, mesh size regulates the steric interactions between the drugs and the polymer network and therefore determines the rate of drug diffusion out of the hydrogel—when the mesh size is larger than the drug, diffusion dominates drug release from the hydrogel, diffusion is slowed when the mesh size is close to the size of the drug, and when the mesh size is smaller than the drug size, the drug is physically entrapped within the hydrogel, and it must be released by a mechanism such as degradation, deformation, or swelling.¹⁵²

MMRs composed of stimulus-responsive hydrogels can leverage drug-delivery research using liposomes, membranes, and block copolymers.^{22,153–155} Hydrogels possess the ability to change their shape and volume, by swelling (or deswelling) in response to a stimulus, thereby facilitating a rapid method of on-demand drug release. In particular, pH-responsive hydrogels contain ionic networks, which, upon exposure to aqueous solutions with an appropriate pH and ionic strength, can cause swelling due to the electrostatic repulsion of the ionized pendant groups.^{156,157} This swelling/deswelling mechanism can mediate drug delivery, as swollen hydrogels have larger meshes, thereby increasing the diffusion of the encapsulated drug out of the hydrogel, compared to unswollen hydrogels with smaller meshes. Alternatively, thermoresponsive hydrogels mediate drug delivery by undergoing a sol-gel phase change above the lower critical solution temperature (LCST) or below the upper critical solution temperature (UCST). For example, below the LCST, thermoresponsive poly(N-isopropylacrylamide) (pNIPAAm) swells, and above the LCST, a shift in aqueous solubility causes the polymer to precipitate out of the solution, resulting in deswelling of the hydrogel through the expulsion of the fluid and the encapsulated drug out of the hydrogel. While these materials have been used alone to design responsive MMRs, they can also couple to other hydrogels with different swelling properties, such that the two hydrogels swell or contract differently in response to a stimulus, thereby causing the structure to fold, in order to achieve triggered drug delivery by releasing compartmentalized cargo.^{123,130}

3. Delivery of cells and large cargo

While many MMR demonstrations involving delivery have emphasized small molecules, recent applications increasingly show the potential of MMRs as delivery devices for larger payloads. While small molecules can simply be encapsulated within the meshes of hydrogels, MMRs designed to transport larger cargo such as cells require other strategies, such as devices with inner compartments,^{123,158,159} or the use of hydrogels fabricated with interconnected micropores.²³ Ultrasound-powered microrods can dynamically load and transport magnetic microspheres or a range of other payloads which are similarly dependent on compatible surface markers. With these larger payloads, it is significant to consider the effect of drag forces, which

increase with the addition of a relatively sizable payload and can be modeled using the Stokes equation

$$F_D = \frac{2\pi\mu Lv}{\ln \frac{L}{r} - 0.5}, \quad (13)$$

where μ is the viscosity of the fluid, L is the length of the nanorod, v is the velocity of the micromotor, and r is the microrod's radius.⁹⁶ While the ability of microrods to functionally tow payloads up to the cellular scale ($\sim 16 \mu\text{m}$) has been demonstrated within *in vitro* environments, it has yet to be shown in blood, where the fluid velocity poses additional challenges for both payload binding and for device velocity.¹⁶⁰

4. Microgrippers

Microgrippers are a unique set of MMRs which are capable of securely grasping a tissue or a cargo, in order to stay immobilized at a desired location or perform functionalities such as surgical tissue excision. However, these devices require mechanical robustness, such as high strength and toughness, to ensure that the device does not deform or fracture while gripping on to its target site. Groups have adopted various strategies to improve the strength of hydrogel-based microgrippers, in order to more robustly latch on to cells and tissue *in vivo* without damaging the tissue, such as the incorporation of poly(propylene fumarate) to pNIPAAm-AAc microgrippers,¹⁴² or interlocking mechanisms with shape-memory properties.¹⁴³ The strength of hydrogels can also be increased through the incorporation of NPs such as carbon nanotubes or ferritin, to form nanocomposites with improved mechanical properties. For example, Wang *et al.* reinforced the poly(N-hydroxyethyl acrylamide) (PHEAm) layer of a pHEAm-pNIPAAm hydrogel bilayer with strengthening cellulose crystal nanocrystals (CNCs) or CNCs with methacrylamide moieties to improve the loading capacity of the hydrogel bilayer.¹⁴⁴ A method to increase toughness is through the use of double network hydrogels, in which two interpenetrating networks are crosslinked separately, which can increase the energy dissipation energy of the hydrogel, as well as its toughness.¹⁶¹

D. Biocompatibility

Finally, since MMRs may be in contact with biological fluids or tissue for potentially long time periods during *in vivo* applications, it is critical that they are biocompatible. In one definition of biocompatibility, the devices should carry out a specific application, with an appropriate host response.¹⁶² Biological responses to implants initially consist of inflammatory and wound healing responses, but in the presence of a foreign body that cannot be phagocytosed by macrophages (devices $< 10 \mu\text{m}$), wound healing evolves into a foreign body reaction (FBR), in which macrophages and monocytes fuse to form foreign body giant cells and is followed by fibrous encapsulation of the foreign body.^{163,164} This can have significant unintended consequences, such as compromised patient safety (biosafety) and compromised device functionality (biofunctionality).¹⁶⁵ However, as demonstrated in other fields such as tissue engineering^{152,166,167} and bioelectronics,^{161,168} the severity of the FBR, which is typically measured by the extent of fibrous encapsulation, can be modulated through careful device material selection and design. Specifically, the use of soft materials, with carefully tuned material properties, can enable device functionality for the intended duration, without causing harm to the patient. Here, we

will discuss how material properties, as well as device properties, can be leveraged to further modulate the FBR, thereby increasing the overall biocompatibility of the MMR (Table IV). The design of soft MMRs can also apply much of the research from tissue engineering or bioelectronics to develop biocompatible soft implants at the microscale.

1. Mechanical compatibility

The elastic modulus of a material describes its ability to resist elastic deformation when subjected to a load and is often used to describe the stiffness of a material. Unlike hard, rigid materials, which have elastic moduli on the order of >1GPa,³³ the stiffness of hydrogels can be tuned from 0.5 kPa to 5 MPa¹⁵² to match the stiffness of the surrounding biological tissue, which is referred to as compliance matching, and can enhance the biocompatibility of a device. Stiffer materials generate high stress concentrations that can cause tissue damage, as well as mechanical damage to the device, whereas soft, deformable devices with elastic moduli similar to the surrounding tissue can cause reduced tissue damage due to the ability to evenly distribute the stress over the contact area.^{33,177} Although not at the microscale, the consequences of mismatched mechanical properties between the tissue and the implanted device with respect to device functionality have been demonstrated thoroughly with neural implants such as electrodes. Implantation of conventional metal or silica neural electrodes with $E > 1\text{GPa}$ into the neural tissue with $E < 100\text{ kPa}$ causes increased brain micromotions, which subsequently leads to increased local strain and local mechanical damage, which drives glial scar (analogous to the fibrous capsule in non-neural environments) formation.¹⁷⁰ The presence of the scar tissue around the implant increases interfacial impedance and reduces stimulation and recording efficacy due to the increase in tissue-electrode distance,

thereby compromising device functionality and causing implant failure.¹⁶⁸ Spencer *et al.*¹⁷⁰ and Rao *et al.*¹⁷⁸ both demonstrated that coating hard, rigid electrodes with soft, polyethylene glycol (PEG)-based hydrogels, which have similar mechanical properties as neural tissue, can reduce glial scarring and implant failure by reducing the level of strain experienced by the brain tissue due to micromotions. In general, the use of soft materials, whose elastic moduli can be tuned to match that of the surrounding tissue (i.e., $E_{\text{brain}} = 5\text{ kPa}$,¹⁷⁰ $E_{\text{cancellous bone}} < 3\text{ GPa}$,¹⁷⁹ $E_{\text{cornea}} = 6\text{ MPa}$ ¹⁸⁰), can minimize the impairment of device functionality as well as the potential for tissue damage or irritation.

Another mechanical property that can impact device biocompatibility is stretchability. As demonstrated with implantable electrodes, differences in stretchability or bending stiffness between tissue and hard, rigid electrodes can cause delamination and impede functionality.¹⁶⁸ Although decreasing the thickness of rigid materials can improve device stretchability and conformability, they can still fail to deform with the underlying tissue and limit the motion of the underlying tissue, causing tissue damage and neuroinflammation.^{181,182} Mineev *et al.* demonstrated that subdural spinal cord implants composed of soft materials resulted in significantly less neuroinflammation in comparison to implants composed of stiff materials.¹⁸²

2. Porosity

Nonporous hydrogels contain nanosize openings (meshes) between polymer chains, whereas porous hydrogels also contain interconnected micro-sized pores, which can affect the physical properties of the hydrogel, as well as its biocompatibility. The impact of microporosity on the biocompatibility of hard implants was assessed by Sharkawy *et al.*¹⁷¹ and Ward *et al.*,¹⁷² who both demonstrated that

TABLE IV. Biocompatibility. Description of the effect of material and device properties (stiffness, porosity, biodegradability, geometry, and size) on fibrotic scarring of implanted device and the resulting effect of scarring on device functionality. These material and device properties can be tuned to maximize biocompatibility and maintain device functionality.

Property of material or device	Effect on scarring		Impact of scarring on functionality	References
	Increased	Decreased		
Stiffness	Stiff	Soft	Higher electrical impedance across a tissue interface due to increased scarring from stiff neural electrodes results in reduced recording and stimulation efficiency	168–170
Porosity	Nonporous (more dense)	Porous (less dense)	Reduced diffusivity of analyte to be sensed or released cargo	171 and 172
Biodegradability	Nonbiodegradable or slowly degrading	Biodegradable or fast degrading	Reduced mass transfer between implants and surrounding tissue	173–175
Geometry and size	Small sphere (0.5 mm diameter, alginate)	Large sphere (1.5 mm diameter, alginate)	Reduced duration of control by encapsulated islet cells over blood glucose levels	176
	Large cylinder (2 mm diameter, polyurethane)	Small cylinder (0.3 mm diameter, polyurethane)	No specifically demonstrated impact on functionality	172

nonporous implants were surrounded by a denser fibrous capsule than porous implants. A consequence of the denser capsule is the reduced diffusivity of small molecules through the capsule, which could inhibit the functionality of implantable sensors or on-demand drug-delivery devices. The Ratner group studied the effect of different pore sizes on the resultant fibrotic response of implantable scaffolds and demonstrated that poly(2-hydroxyethyl methacrylate-co-methacrylic acid) (PMMA) hydrogel scaffolds with smaller pores (diameter 30–40 μm) had reduced fibrotic scarring due to a shift in macrophage phenotype toward the anti-inflammatory M2 state, in comparison to scaffolds with larger pores.^{183–185}

3. Degradability

A direct means to enhance biocompatibility is to develop rapidly biodegradable devices (with biocompatible degradation products), as the duration of granulation tissue development, FBR, and resulting fibrous encapsulation are all influenced by the rate of degradation of the implant.¹⁸⁶ In general, slowly degrading hydrogels, which remain in the body for longer periods of time, can induce a longer-lasting immune response with fibrous encapsulation or glial scarring, in comparison to quickly degrading hydrogels, which remain in the body for less time.¹⁷³ Thus, although the rate of degradation is tied to the length of time the device is required to remain in the body to complete its intended functionality, it is also important to consider the rate of degradation to improve the biocompatibility of the device. For example, the hydrogel pNIPAAm, previously discussed as a material for thermoresponsive MMRs, has exhibited dampened rates of clinical adoption due to its lack of biodegradability; this trait hinders the material's long-term biocompatibility, as well as the potential for depolymerization of pNIPAAm into its toxic monomeric form. Though involving complicated chemistry, efforts have been made to fabricate pNIPAAm with various crosslinkers to enable biodegradation into known, non-toxic degradation products.¹⁸⁷ The use of biodegradable pNIPAAm in MMRs could alleviate some of the concerns related to the long-term presence of pNIPAAm-based devices.

4. Geometry and size

The geometry and size of implantable devices are properties of the implant which can also dictate the degree of the FBR against a device. Seminal studies by Malaga *et al.*¹⁸⁸ and Salthouse *et al.*¹⁸⁹ demonstrated that polymeric devices with smooth surfaces are likely to be more biocompatible than devices with sharp edges. Others have since studied whether an ideal geometry and size of the device can minimize the FBR. For example, although not a hydrogel, Ward *et al.* implanted cylindrical polyurethane devices with a diameter of 300 or 2000 μm into rats and demonstrated that the large implant induced a thicker fibrotic capsule 7 weeks post implantation.¹⁷² Conversely, Veiseh *et al.* demonstrated that intraperitoneal injection of alginate hydrogel microspheres (ranging from 300 to 1900 μm in diameter) into wild-type mice resulted in a significantly reduced FBR and fibrotic capsule around the larger spheres in comparison to the smaller spheres, at the 7 week time point.¹⁷⁶ Although MMRs are typically below 1 mm, these studies highlight that both geometry and size can be tuned to enhance biocompatibility.

5. Other components within MMRs

While the bulk material of MMRs has a significant role in the immunogenicity of implanted devices, it is also necessary to consider the biocompatibility of the other components encapsulated within, or coated atop the device, to enable control, locomotion, or functionality of the devices. For example, a common means of achieving the locomotion of MMRs is through magnetic control, which is typically achieved through the coating of hard, rigid MMRs with nickel, or through the encapsulation of magnetic (iron oxide) NPs within soft MMRs, both of which also need to be considered in determining the biological response against the overall MMR. Though iron oxide NPs are considerably more biocompatible than nickel, as Ferumoxytol has received FDA approval for specific indications,¹⁹⁰ there are still concerns over the immunogenicity of magnetic NPs, which are nonbiodegradable and would therefore remain in the body upon degradation of the bulk soft material. The biocompatibility of iron oxide NPs is largely dependent on its composition and surface coatings; certain compositions can be efficiently phagocytosed by immune cells in the liver, whereas other compositions remain in the body for longer, which can cause toxicities via the induction of oxidative stress. Furthermore, the concentration of localized iron oxide NPs can have toxic effects when accumulated in sufficiently high concentrations at localized areas.¹⁹¹ In order to circumvent toxicities related to magnetic NPs that remain in the body following localization and degradation of gelatin-based MMRs, Kim *et al.* proposed the retrieval of the magnetic NPs by using the electromagnetic actuation system used to move the MMRs.¹⁹²

Biocompatibility is a critical requirement of MMRs, which, for the most part, has been overlooked, in favor of achieving functionality instead. In general, tests for biocompatibility have been extremely rudimentary and simply involve *in vitro* cytotoxicity assays (Table V). International standards, such as ISO 10993—Biological Evaluation of Medical Devices, have been developed to guide the testing of biocompatibility of different types of medical devices. Given the unique effect of forces and environmental conditions in the low-Re world of micro-devices, MMRs may require additional biological considerations and biocompatibility demonstrations, above the metrics of the ISO guidelines, to ensure patient safety. Finally, soft materials can be composed of natural or synthetic polymers. Although synthetic materials can be more precisely defined and more tightly controlled in terms of mechanical properties, porosity, and degradation to enhance biocompatibility as described above, natural polymers (e.g., gelatin, collagen) can potentially be autologously harvested, such that devices are composed of patient-specific materials which would not be considered foreign upon implantation.¹³⁷

III. SYSTEM INTEGRATION

Many studies have demonstrated the proof of concept of individual design components. However, reaching *in vivo* impact will require the integration of four different design elements, as reflected by appropriate device geometry to achieve locomotion through target environments, responsiveness to a relevant control modality, ability to perform specific functionalities at target sites, and appropriate biocompatibility over the duration of use. Prior works in these four areas have emphasized the following solutions. Methods for locomotion have included bioinspired designs, namely, microswimmers which mimic bacteria, but this design exhibits limited capacities in terms of payload size and ability to maneuver outside of a purely fluid environment. For

TABLE V. Integration of hydrogel-based MMRs. Examples of integrated soft MMRs which satisfy all four of the design characteristics of movement, control, functionality, and biocompatibility. All of these devices are at least partially magnetically controlled. Future diversity in control modalities could expand the range of functionalities and overcome some of the listed limitations. Reprinted with permission from Ceylan *et al.*, ACS Nano **13**(3), 3353–2262 (2019). Copyright 2019 American Chemical Society. Further permissions related should be directed to the ACS. Reprinted with permission from Kuo *et al.*, Sens. Actuators, A **211**, 121–130 (2014). Copyright (2014) Elsevier. Reprinted with permission from Li *et al.*, Smart Mater. Struct. **25**(2), 027001 (2016). Copyright 2016 IOP Publishing. Reproduced with permission from Park *et al.*, Adv. Healthcare Mater. **8**, 1900213 (2019). Copyright 2019 Wiley. Reprinted in part with permission from Fusco *et al.*, Adv. Mater. **26**(6), 952–957 (2014). Copyright 2013 Wiley. Reprinted with permission from Kobayashi *et al.*, ACS Appl. Mater. Interfaces **11**(1), 151–159 (2018). Copyright 2018 American Chemical Society.

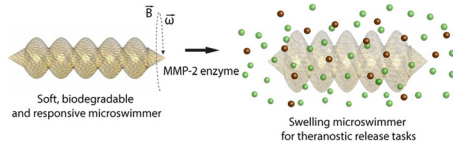
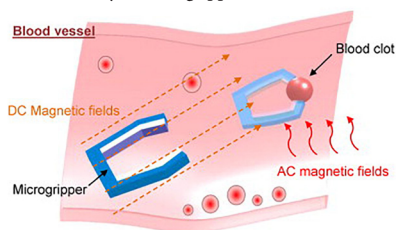
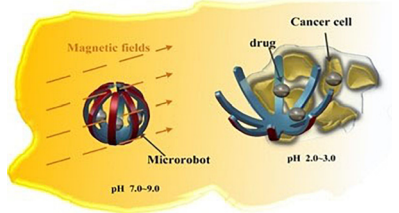
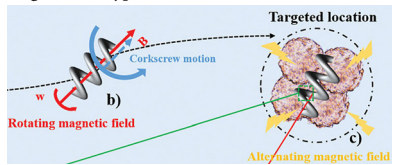
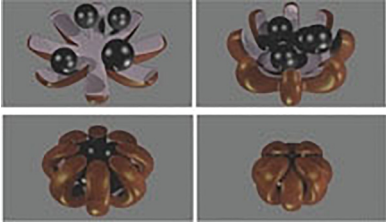
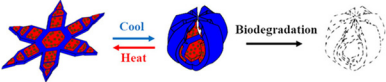
Device	Material	Fabrication method	Locomotion		Controller mechanism	Functionality	Biocompatibility tests	References
			Geometry	Intended location				
Biodegradable microswimmer (d1) 	Gelatin methacrylate [matrix metalloproteinase 2 (MMP2)-responsive] with iron oxide NPs	3D printing via two-photon polymerization	Cylindrical core wrapped by a double helix, with cones at the ends	Tumor site	Extracorporeal (magnetic modality) Intrinsic (sensing of MMP2 levels)	Sensing (MMP2 levels) Delivery of drugs (targeted release of drugs and NPs coated with antibodies to tag tumor cells)	<i>In vitro</i> cytotoxicity (coculture of microswimmer degradation products with cancer cell line for 24 h)	137
Foldable bilayer microgripper (d2) 	pNIPAAm (thermoreponsive) with multiwalled carbon nanotubes and iron oxide NPs	Soft lithography	Horseshoelike	Through blood vessels	Extracorporeal (AC and DC magnetic modalities)	Gripping of tissue (targeted opening or closing of grippers to pick up or release blood clot)	None	145
Foldable bilayer with internal compartment (d3) 	Poly (2-hydroxyethyl methacrylate) (pH-responsive) and polyethylene glycol diacrylate (PEGDA) with iron oxide NPs	Photolithography	Spherelike	Through blood vessels to tumor site	Extracorporeal (magnetic modality) Intrinsic (sensing of pH levels)	Sensing (pH levels) Delivery of drugs (targeted release of microbeads loaded with an anticancer drug)	<i>In vitro</i> cytotoxicity (coculture of microrobots with cancer cell line for 24 h)	130
Degradable hyperthermia microrobot (d4) 	PEGDA and pentaerythritol with iron oxide NPs	Two-photon polymerization	Helical	Tumor site	Extracorporeal (rotating and alternating magnetic modality)	Drug delivery (targeted release of anti-cancer drug) Thermal ablation	<i>In vitro</i> cytotoxicity (coculture of microrobots (without anti-cancer drug) with cancer cell line for 48 h)	200

TABLE V. (Continued.)

Device	Material	Fabrication method	Locomotion		Controller mechanism	Functionality	Biocompatibility tests	References
			Geometry	Intended location				
Foldable bilayer with internal compartment (d5) 	PEGDA and pNIPAAm-graphene oxide nanocomposite (thermo-responsive) with alginate microparticles encapsulating iron oxide NPs	Photolithography	Spherelike (jellyfish- or Venus fly traplike structures)	Remote parts of the body (e.g., hepatic artery)	Extracorporeal (magnetic modality) Extracorporeal (NIR modality)	Drug or cell delivery (targeted release of alginate microparticles encapsulating cells or drugs)	<i>In vitro</i> cytotoxicity (coculture of hydrogel bilayers or hydrogel-conditioned medium with fibroblasts for 2 days) <i>In vitro</i> viability of encapsulated mesenchymal stem cells for 7 days	123
Biodegradable foldable bilayer grippers (d6) 	Poly(oligoethylene glycol methyl ether methacrylate ($M_n = 500$)-bis(2-methacryloyl)oxyethyl disulfide) (thermo-responsive) and poly(-acrylamide- N,N' -bis(acyloyl)cystamine) with iron oxide NPs	Photolithography	Spherelike	Through tissue	Extracorporeal (magnetic modality) Intrinsic (sensing of temperature)	Sensing (temperature) Gripping of tissue (targeted closing of grippers to excise cells)	<i>In vitro</i> cytotoxicity (coculture of grippers with endothelial cell line for 3 days)	201

feedback and control, most demonstrations with externally controlled modalities employ magnetic methods, including electromagnetic coils from a custom or an MRI system and permanent magnets; typically, the corresponding implanted MMRs have embedded magnetic NPs to ensure responsiveness. For functionality, while MMRs have been proposed as potential treatment options for a variety of conditions, the field thus far has largely emphasized methods of drug delivery. Finally, for biocompatibility, a large array of MMRs are fabricated from rigid materials and incorporate magnetic coatings, thereby increasing the likelihood of a fibrotic tissue response that will negate the device's functionality and locomotion principles. Hence, concepts toward integrated MMRs have exhibited one or more limitations, such as settings for locomotion (only one type of tissue or behavior in swarm settings), depth and range of control mechanisms, biocompatibility, and biodegradability.^{193–195} Very few MMRs have thus far fully integrated control, movement, and medical functionality, particularly for *in vivo* contexts.

Nevertheless, several initial demonstrations have shown significant promise, particularly as methods of triggered drug delivery (which can reduce the toxicities associated with systemic drug delivery) and targeted cell therapies (which can improve upon the poor homing of cells to the target location following systemic injections). The integration of controlled locomotion with the ability to perform functionalities by sensing the environment and then intervening in some manner could be very valuable. Such a device would be useful for early cancer detection and treatment, where currently, milli-scale devices have been developed to capture cancer cells, such as circulating tumor cells for early cancer detection,¹⁹⁶ or metastatic cells for the early detection of metastatic cancers following the treatment of the primary tumor.^{197,198} These types of devices could potentially be coupled with a mechanism for readout in order to inform a healthcare professional of a potential diagnosis, or with a mechanism to deliver drugs to kill the cells upon capture by the device.

As this field is still at a developing stage and the potential applications for these versatile devices are still being defined, few soft material-based devices have been fully integrated with mechanisms for control, locomotion, and functionality (Table V). Interestingly, there are many commonalities between the majority of these devices in terms of control modalities, mechanisms to achieve functionality, as well as the extent to which these devices have been tested for functionality, locomotion, and biocompatibility. Furthermore, many of these soft MMRs have only undergone very rudimentary *in vitro* cytotoxicity assays and no *in vivo* tests for locomotion, functionality, or biocompatibility. As well as incorporating more diverse mechanisms for control over locomotion and functionality, much work has to be done to assess overall biocompatibility, locomotion, and functionality of integrated devices to ensure that they are able to perform as intended, regardless of the many obstacles present *in vivo*.

Furthermore, the full life span of integrated devices must be considered when intended for *in vivo* applications. Depending on the exact scale and mobility modality of a soft MMR, it will likely enter the body via injection and migrate from a peripheral vessel to the intended application site. Depending on the intended functionality and the extent of biocompatibility, the device may need to be removed, such as to screen any collected cells or other significant biomarkers; ideally, the MMRs could also be removed via injection. An alternative method of addressing the end of a device's life span is that the device

biodegrades, either naturally or via stimulation such as by ultrasound cavitation.¹⁹⁹ Such longer-term consideration of the use case for MMRs is another next step of consideration for integration.

Finally, when considering the possibility of MMRs for long-term use, or potentially repeatedly triggered use within the body, it is significant to consider methods of tracking and imaging, either in combination or in parallel with the control method for movement and functionality. While current applications are primarily designed for either immediate and in-patient situations or are intended to be repeatedly triggerable but are relatively stationary, MMRs could eventually remain dormant but circulating in the body for significant periods between usage. In such instances, tracking mechanisms, such as RF or fluorescence imaging, may be critical to relocate devices at the onset of each usage period.

IV. FUTURE PERSPECTIVES AND CONCLUSION

From recent research across multiple design elements, a coherent paradigm for how to build an integrated MMR is emerging. At the moment, emphasis has been placed on locomotion and drug-delivery functions. For materials, in addition to microelectronics and biohybrid designs, soft materials are increasingly being developed and shaped for novel uses. In the future, to achieve precise operation, wireless communication modalities will be increasingly integrated into MMRs as part of well-developed feedback and control systems—for data acquisition, communication, and control—as seen in increasingly prevalent macroscale robotic systems. On the other hand, unlike macroscale robotic systems, by virtue of the human body environment, as well as constraints placed on the size and power of the communication elements, the wireless communication modalities will likely be different.

Another likely trend is the increasing incorporation of machine learning, such that the devices can “learn” from an environment,²⁰² which can lead to closed-loop operation and increasing autonomous behavior. An early demonstration is an MEMS circuit that senses shear stress, analyzes the signal via neural network, and then reduces the drag of the device by adjusting microactuators.²⁰² More recently, MEMS devices, namely, gyroscopes and accelerometers, have become commonplace consumer products; the integration of machine learning with such wearable devices enables additional training functionalities, such as for predicting risk factors for obesity based on daily calorie and step count.²⁰³ In addition, machine learning has begun to assist in radiological imaging tasks, such as detection, diagnosis, and therapeutic response.²⁰⁴ In the future, the integration of machine learning with implantable devices and microrobots is likely to become increasingly relevant to achieve unprecedented functions.

With such recent research and emerging trends, the tantalizing but technically demanding vision of MMRs is coming closer. The successful development of MMRs could enable a medical future with minimally invasive interventions (and corresponding reductions in the risk of infection, recovery time, pain, and other complications) and novel approaches for the maintenance of wellness and improvement in overall human performance.

ACKNOWLEDGMENTS

The authors acknowledge NSF Grant No. ECCS-1509748. R.D.F. acknowledges support from the National Center for Advancing Translational Sciences, National Institutes of Health, through Grant No. TL1TR001875. The content is solely the responsibility of the authors and does not necessarily represent the funding agencies.

REFERENCES

- ¹C. Toumey, *Nat. Nanotechnol.* **4**, 783 (2009).
- ²M. Sitti, H. Ceylan, W. Hu, J. Giltinan, M. Turan, S. Yim, and E. Diller, *Proc. IEEE Inst. Electr. Electron. Eng.* **103**, 205–224 (2015).
- ³S. Ornes, *Proc. Natl. Acad. Sci.* **114**, 12356–12358 (2017).
- ⁴B. J. Nelson, I. K. Kaliakatos, and J. J. Abbott, *Annu. Rev. Biomed. Eng.* **12**, 55–85 (2010).
- ⁵C. Hu, S. Pané, and B. J. Nelson, *Annu. Rev. Control, Rob., Auton. Syst.* **1**, 53–75 (2018).
- ⁶M. Sitti, *Mobile Microrobotics* (MIT Press, 2017).
- ⁷R. Bogue, *Ind. Robot* **35**, 294–299 (2008).
- ⁸K. E. Drexler, *Proc. Natl. Acad. Sci.* **78**, 5275–5278 (1981).
- ⁹K. Lund, A. J. Manzo, N. Dabby, N. Michelotti, A. Johnson-Buck, J. Nangreave, S. Taylor, R. Pei, M. N. Stojanovic, and N. G. Walter, *Nature* **465**, 206 (2010).
- ¹⁰A. W. Feinberg, *Annu. Rev. Biomed. Eng.* **17**, 243–265 (2015).
- ¹¹D. Rus and M. T. Tolley, *Nature* **521**, 467 (2015).
- ¹²S. Bauer, S. Bauer-Gogonea, I. Graz, M. Kaltenbrunner, C. Keplinger, and R. Schwödiauer, *Adv. Mater.* **26**, 149–162 (2014).
- ¹³C. Chautems, B. Zeydan, S. Charreyron, G. Chatzipirpiridis, S. Pane, and B. J. Nelson, *Eur. J. Cardio-Thorac. Surg.* **51**, 405–407 (2017).
- ¹⁴A. Shah, J. D. Harper, B. W. Yountz, Y.-N. Wang, M. Paun, J. C. Simon, W. Lu, P. J. Kaczowski, and M. R. Bailey, *J. Urol.* **187**, 739–743 (2012).
- ¹⁵D. Holligan, G. Gillies, and J. Dailey, *Nanotechnology* **14**, 661 (2003).
- ¹⁶A. W. Flake, *J. Physiol.* **547**, 45–51 (2003).
- ¹⁷S. Kim, F. Qiu, S. Kim, A. Ghanbari, C. Moon, L. Zhang, B. J. Nelson, and H. Choi, *Adv. Mater.* **25**, 5863–5868 (2013).
- ¹⁸X. Yang, H. Wang, L. Yuan, N. Du, and Z. Hou, editors, “Minimally invasive vascular interventional surgical robot system,” in *2011 IEEE International Conference on Mechatronics and Automation* (IEEE, 2011).
- ¹⁹R. Bashir, *Adv. Drug Delivery Rev.* **56**, 1565–1586 (2004).
- ²⁰M. Leonardi, P. Leuenberger, D. Bertrand, A. Bertsch, and P. Renaud, *Invest. Ophthalmol. Visual Sci.* **45**, 3113–3117 (2004).
- ²¹P. Cong, W. H. Ko, and D. J. Young, *IEEE Sens. J.* **10**, 243–254 (2010).
- ²²“Toward targeted retinal drug delivery with wireless magnetic microrobots,” in *2008 IEEE/RSJ International Conference on Intelligent Robots and Systems*, edited by G. Dogangil, O. Ergeneman, J. J. Abbott, S. Pané, H. Hall, S. Muntwyler, and B. J. Nelson (IEEE, 2008).
- ²³G. Go, J. Han, J. Zhen, S. Zheng, A. Yoo, M.-J. Jeon, J.-O. Park, and S. Park, *Adv. Healthcare Mater.* **6**, 1601378 (2017).
- ²⁴K. Kalantar-Zadeh, K. J. Berean, N. Ha, A. F. Chrimes, K. Xu, D. Grando, J. Z. Ou, N. Pillai, J. L. Campbell, and R. Brkljača, *Nat. Electron.* **1**, 79 (2018).
- ²⁵X. Liu, C. Steiger, S. Lin, G. A. Parada, J. Liu, H. F. Chan, H. Yuk, N. V. Phan, J. Collins, and S. Tamang, *Nat. Commun.* **10**, 493 (2019).
- ²⁶“Injectable, controllable, and degradable origami robot for patching stomach wounds,” in *2016 IEEE International Conference on Robotics and Automation (ICRA)*, edited by S. Miyashita, S. Guitron, K. Yoshida, S. Li, D. D. Damian, and D. Rus (IEEE, 2016).
- ²⁷A. Abramson, E. Caffarel-Salvador, M. Khang, D. Dellal, D. Silverstein, Y. Gao, M. R. Frederiksen, A. Vegge, F. Hubálek, and J. J. Water, *Science* **363**, 611–615 (2019).
- ²⁸M. R. Basar, F. Malek, K. M. Juni, M. S. Idris, and M. I. M. Saleh, *Int. J. Antennas Propag.* **2012**, 807165.
- ²⁹L. Ricotti, B. Trimmer, A. W. Feinberg, R. Raman, K. K. Parker, R. Bashir, M. Sitti, S. Martel, P. Dario, and A. Mencias, *Sci. Rob.* **2**, eaaq0495 (2017).
- ³⁰L. Schwarz, M. Medina-Sánchez, and O. G. Schmidt, *Appl. Phys. Rev.* **4**, 031301 (2017).
- ³¹D. B. Weibel, P. Garstecki, D. Ryan, W. R. DiLuzio, M. Mayer, J. E. Seto, and G. M. Whitesides, *Proc. Natl. Acad. Sci.* **102**, 11963–11967 (2005).
- ³²F. Ilievski, A. D. Mazzeo, R. F. Shepherd, X. Chen, and G. M. Whitesides, *Angew. Chem. Int. Ed.* **50**, 1890–1895 (2011).
- ³³C. Majidi, *Soft Rob.* **1**, 5–11 (2013).
- ³⁴W. Hu, G. Z. Lum, M. Mastrangeli, and M. Sitti, *Nature* **554**, 81 (2018).
- ³⁵M. Choi, M. Humar, S. Kim, and S. H. Yun, *Adv. Mater.* **27**, 4081–4086 (2015).
- ³⁶N. Sood, A. Bhardwaj, S. Mehta, and A. Mehta, *Drug Delivery* **23**, 748–770 (2016).
- ³⁷J.-Y. Sun, X. Zhao, W. R. Illeperuma, O. Chaudhuri, K. H. Oh, D. J. Mooney, J. J. Vlassak, and Z. Suo, *Nature* **489**, 133 (2012).
- ³⁸S. Y. Chin, Y. C. Poh, A.-C. Kohler, J. T. Compton, L. L. Hsu, K. M. Lau, S. Kim, B. W. Lee, F. Y. Lee, and S. K. Sia, *Sci. Rob.* **2**, eaah6451 (2017).
- ³⁹N. Tejaviyulya, D. A. Colburn, F. A. Marcogliese, K. Yang, V. Guo, S. Chowdhury, M. N. Stojanovic, and S. K. Sia, *Towards Intradermal Health Monitoring* (iScience, 2019).
- ⁴⁰“Spiral-type micro-machine for medical applications,” in *MHS2000 Proceedings of 2000 International Symposium on Micromechatronics and Human Science (Cat No 00TH8530)*, edited by K. Ishiyama, K. Arai, M. Sendoh, and A. Yamazaki (IEEE, 2000).
- ⁴¹R. Cortez, L. Fauci, N. Cowen, and R. Dillon, *Comput. Sci. Eng.* **6**, 38 (2004).
- ⁴²P. Fischer and A. Ghosh, *Nanoscale* **3**, 557–563 (2011).
- ⁴³E. M. Purcell, *Am. J. Phys.* **45**, 3–11 (1977).
- ⁴⁴H. Li, J. Tan, and M. Zhang, *IEEE Trans. Autom. Sci. Eng.* **6**, 220–227 (2009).
- ⁴⁵E. Diller and M. Sitti, *Found. Trends Rob.* **2**, 143–259 (2013).
- ⁴⁶S. Martel, J.-B. Mathieu, O. Felfoul, A. Chanu, E. Aboussouan, S. Tamaz, P. Pouponneau, L. H. Yahia, G. Beaudoin, and G. Soulez, *Appl. Phys. Lett.* **90**, 114105 (2007).
- ⁴⁷T. L. Daniel, *Am. Zool.* **24**, 121–134 (1984).
- ⁴⁸D. E. Alexander, *Nature’s Machines: An Introduction to Organismal Biomechanics* (Academic Press, 2017).
- ⁴⁹L. Arcese, M. Fruchard, and A. Ferreira, *IEEE Trans. Biomed. Eng.* **59**, 977–987 (2012).
- ⁵⁰E. Lauga, *Phys. Rev. E* **75**, 041916 (2007).
- ⁵¹E. Lauga, *Phys. Fluids* **19**, 083104 (2007).
- ⁵²E. Lauga and T. R. Powers, *Rep. Prog. Phys.* **72**, 096601 (2009).
- ⁵³O. Raz and J. Avron, *New J. Phys.* **9**, 437 (2007).
- ⁵⁴A. Najafi and R. Golestanian, *J. Phys.: Condens. Matter* **17**, S1203 (2005).
- ⁵⁵H. W. Huang, F. E. Uslu, P. Katsamba, E. Lauga, M. S. Sakar, and B. J. Nelson, *Sci. Adv.* **5**, eaau1532 (2019).
- ⁵⁶B. de Lima Bernardo and F. Moraes, *Am. J. Phys.* **79**, 736–740 (2011).
- ⁵⁷H. Wang and M. Pumera, *Adv. Funct. Mater.* **28**, 1705421 (2018).
- ⁵⁸K. J. Rao, F. Li, L. Meng, H. Zheng, F. Cai, and W. Wang, *Small* **11**, 2836–2846 (2015).
- ⁵⁹H.-W. Huang, M. S. Sakar, A. J. Petruska, S. Pané, and B. J. Nelson, *Nat. Commun.* **7**, 12263 (2016).
- ⁶⁰G. Langousis and K. L. Hill, *Nat. Rev. Microbiol.* **12**, 505 (2014).
- ⁶¹F. Becker, K. Zimmermann, T. Volkova, and V. T. Minchenya, *Regular Chaotic Dyn.* **18**, 63–74 (2013).
- ⁶²M. T. Hou, H.-M. Shen, G.-L. Jiang, C.-N. Lu, I.-J. Hsu, and J. A. Yeh, *Appl. Phys. Lett.* **96**, 024102 (2010).
- ⁶³H.-W. Tung, K. E. Peyer, D. F. Sargent, and B. J. Nelson, *Appl. Phys. Lett.* **103**, 114101 (2013).
- ⁶⁴“Micro-assembly and modeling of the liquid microworld: The PRONOMA project,” in *Proceedings of the IEEE/RSJ International Conference on Intelligent Robots and Systems*, edited by M. Gauthier, S. Régnier, B. Lopez-Walle, E. Gibeau, P. Rougeot, D. Hérriban, and N. Chaillet (2007).
- ⁶⁵S. Floyd, C. Pawashe, and M. Sitti, *IEEE Trans. Rob.* **25**, 1332–1342 (2009).
- ⁶⁶“Modeling of electrostatic forces induced by chemical surface functionalisation for microrobotics applications,” in *2013 IEEE/RSJ International Conference on Intelligent Robots and Systems*, edited by A. Cot, J. Dejeu, S. Lakard, P. Rougeot, and M. Gauthier (IEEE, 2013).
- ⁶⁷R. Zhao, Y. Kim, S. A. Chester, P. Sharma, and X. Zhao, *J. Mech. Phys. Solids* **124**, 244–263 (2019).
- ⁶⁸W. Lee, N. Kalashnikov, S. Mok, R. Halaoui, E. Kuzmin, A. J. Putnam, S. Takayama, M. Park, L. McCaffrey, and R. Zhao, *Nat. Commun.* **10**, 144 (2019).
- ⁶⁹W. Hong, X. Zhao, J. Zhou, and Z. Suo, *J. Mech. Phys. Solids* **56**, 1779–1793 (2008).
- ⁷⁰C. Bi, M. Guix, B. Johnson, W. Jing, and D. Capperli, *Micromachines* **9**, 68 (2018).

- ⁷¹“Modeling of van der Waals forces during the assembly of micro devices,” in *2006 IEEE International Conference on Automation Science and Engineering*, edited L. Zhang, J. Cecil, D. Vasquez, J. Jones, and B. Garner (IEEE, 2006).
- ⁷²J. K. Dhont, *An Introduction to Dynamics of Colloids* (Elsevier, 1996).
- ⁷³H. Xie, M. Sun, X. Fan, Z. Lin, W. Chen, L. Wang, L. Dong, and Q. He, *Sci. Rob.* **4**, eaav8006 (2019).
- ⁷⁴D. Cappelleri, D. Efthymiou, A. Goswami, N. Vitoroulis, and M. Zavlanos, *Int. J. Adv. Rob. Syst.* **11**, 150 (2014).
- ⁷⁵K. Belharet, D. Folio, and A. Ferreira, *IEEE Trans. Biomed. Eng.* **60**, 994–1001 (2012).
- ⁷⁶M. Fruchard, L. Arcese, and E. Courtial, *IEEE Trans. Rob.* **30**, 93–102 (2013).
- ⁷⁷R. G. Simmons, *IEEE Trans. Rob. Autom.* **10**, 34–43 (1994).
- ⁷⁸M. Hoy, A. S. Matveev, and A. V. Savkin, *Robotica* **33**, 463–497 (2015).
- ⁷⁹K. J. Aström and R. M. Murray, *Feedback Systems: An Introduction for Scientists and Engineers* (Princeton University Press, 2010).
- ⁸⁰“Sensors for micro bio robots via synthetic biology,” in *2014 IEEE International Conference on Robotics and Automation (ICRA)*, E. B. Steager, D. Wong, D. Mishra, R. Weiss, and V. Kumar (IEEE, 2014).
- ⁸¹M. Okwori, A. Behfarnia, P. Vuka, and A. Eslami, preprint [arXiv:180606163](https://arxiv.org/abs/180606163) (2018).
- ⁸²“An implantable wireless microdosimeter for radiation oncology,” in *2008 IEEE 21st International Conference on Micro Electro Mechanical Systems*, edited by C. Son and B. Ziaie (IEEE, 2008).
- ⁸³“First leaps of an electrostatic inchworm motor-driven jumping microrobot,” in *Micro Electro Mechanical Systems (MEMS)*, edited by J. Greenspun and K. S. Pister (2018).
- ⁸⁴K. Wang, N. G. Horton, K. Charan, and C. Xu, *IEEE J. Sel. Top. Quantum Electron.* **20**, 50–60 (2013).
- ⁸⁵K. Köhrmann, M. Michel, A. Steidler, E. Marlinghaus, O. Kraut, and P. Alken, *BJU Int.* **90**, 248–252 (2002).
- ⁸⁶R. Weissleder, *Nat. Biotechnol.* **19**, 316–317 (2001).
- ⁸⁷U. Walter, M. Kanowski, J. Kaufmann, A. Grossmann, R. Benecke, and L. Niehaus, *Neuroimage* **40**, 551–558 (2008).
- ⁸⁸M. Jang, H. Ruan, B. Judkewitz, and C. Yang, *Opt. Express* **22**, 5787–5807 (2014).
- ⁸⁹J. A. Virmont, “NIR medical imaging: Spatial resolution and discrimination,” *Proc. SPIE* **2389**, 358–365 (1995).
- ⁹⁰T. Xu, W. Gao, L. P. Xu, X. Zhang, and S. Wang, *Adv. Mater.* **29**, 1603250 (2017).
- ⁹¹Z. Izadifar, P. Babyn, and D. Chapman, *Ultrasound Med. Biol.* **43**, 1085–1104 (2017).
- ⁹²A. Raza, U. Hayat, T. Rasheed, M. Bilal, and H. M. Iqbal, *J. Mater. Res. Technol.* **8**, 1497–1509 (2019).
- ⁹³M. P. Kummer, J. J. Abbott, B. E. Kratochvil, R. Borer, A. Sengul, and B. J. Nelson, *IEEE Trans. Rob.* **26**, 1006–1017 (2010).
- ⁹⁴S. Martel, *Int. J. Adv. Rob. Syst.* **10**, 30 (2013).
- ⁹⁵W. Wang, L. A. Castro, M. Hoyos, and T. E. Mallouk, *ACS Nano* **6**, 6122–6132 (2012).
- ⁹⁶V. Garcia-Gradilla, J. Orozco, S. Sattayasamitsathit, F. Soto, F. Kuralay, A. Pourazary, A. Katzenberg, W. Gao, Y. Shen, and J. Wang, *ACS Nano* **7**, 9232–9240 (2013).
- ⁹⁷O. Ordeig, S. Y. Chin, S. Kim, P. V. Chitnis, and S. K. Sia, *Sci. Rep.* **6**, 22803 (2016).
- ⁹⁸M. N. Hoff, A. McKinney IV, F. G. Shellock, U. Rassner, T. Gilk, R. E. Watson, Jr., T. D. Greenberg, J. Froelich, and E. Kanal, *Radiology* **292**, 182742 (2019).
- ⁹⁹“Magnetic control of self-propelled microjets under ultrasound image guidance,” in *5th IEEE RAS/EMBS International Conference on Biomedical Robotics and Biomechanics*, edited by A. Sánchez, V. Magdanz, O. G. Schmidt, and S. Misra (IEEE, 2014).
- ¹⁰⁰B. P. Timko and D. S. Kohane, *Expert Opin. Drug Delivery* **11**, 1681–1685 (2014).
- ¹⁰¹X. Yan, Q. Zhou, M. Vincent, Y. Deng, J. Yu, J. Xu, T. Xu, T. Tang, L. Bian, and Y.-X. J. Wang, *Sci. Rob.* **2**, eaq1155 (2017).
- ¹⁰²G. Chatzipirpiridis, O. Ergeneman, J. Pokki, F. Ullrich, S. Fusco, J. A. Ortega, K. M. Sivaraman, B. J. Nelson, and S. Pané, *Adv. Healthcare Mater.* **4**, 209–214 (2015).
- ¹⁰³“Design and development of a soft magnetically-propelled swimming micro-robot,” in *2011 IEEE International Conference on Robotics and Automation*, edited S. Palagi, V. Pensabene, L. Beccai, B. Mazzolai, A. Menciassi, and P. Dario (IEEE, 2011).
- ¹⁰⁴M. Suter, L. Zhang, E. C. Siringil, C. Peters, T. Luehmann, O. Ergeneman, K. E. Peyer, B. J. Nelson, and C. Hierold, *Biomed. Microdevices* **15**, 997–1003 (2013).
- ¹⁰⁵K. I. Morozov and A. M. Leshansky, *Nanoscale* **6**, 12142–12150 (2014).
- ¹⁰⁶O. Felfoul, A. T. Becker, G. Fagogenis, and P. E. Dupont, *Sci. Rep.* **6**, 33567 (2016).
- ¹⁰⁷E. Diller, J. Giltinan, G. Z. Lum, Z. Ye, and M. Sitti, *Int. J. Rob. Res.* **35**, 114–128 (2016).
- ¹⁰⁸E. A. Neppiras, *Phys. Rep.* **61**, 159–251 (1980).
- ¹⁰⁹D. Vilkomerson and D. Lyons, *IEEE Trans. Ultrason., Ferroelectr., Freq. Control* **44**, 27–35 (1997).
- ¹¹⁰F. Nadal and E. Lauga, *Phys. Fluids* **26**, 082001 (2014).
- ¹¹¹A. A. Doinikov, *Recent Res. Dev. Acoust.* **1**, 39–67 (2003).
- ¹¹²K. A. Garvin, D. C. Hocking, and D. Dalecki, *Ultrasound Med. Biol.* **36**, 1919–1932 (2010).
- ¹¹³R. Habibi, C. Devendran, and A. Neild, *Lab Chip* **17**, 3279–3290 (2017).
- ¹¹⁴D. Kagan, M. J. Benchimol, J. C. Claussen, E. Chuluun-Erdene, S. Esener, and J. Wang, *Angew. Chem. Int. Ed. Engl.* **51**, 7519–7522 (2012).
- ¹¹⁵T. Xu, F. Soto, W. Gao, V. Garcia-Gradilla, J. Li, X. Zhang, and J. Wang, *J. Am. Chem. Soc.* **136**, 8552–8555 (2014).
- ¹¹⁶S. Ahmed, W. Wang, L. Bai, D. T. Gentekos, M. Hoyos, and T. E. Mallouk, *ACS Nano* **10**, 4763–4769 (2016).
- ¹¹⁷T. Laurell, F. Petersson, and A. Nilsson, *Chem. Soc. Rev.* **36**, 492–506 (2007).
- ¹¹⁸X. Zhao, J. Kim, C. A. Cezar, N. Huebsch, K. Lee, K. Bouhadir, and D. J. Mooney, *Proc. Natl. Acad. Sci.* **108**, 67–72 (2011).
- ¹¹⁹A. Sakudo, *Clin. Chim. Acta* **455**, 181–188 (2016).
- ¹²⁰P. Klán, T. Šolomek, C. G. Bochet, A. Blanc, R. Givens, M. Rubina, V. Popik, A. Kostikov, and J. Wirz, *Chem. Rev.* **113**, 119–191 (2013).
- ¹²¹X. Ding, C. H. Liow, M. Zhang, R. Huang, C. Li, H. Shen, M. Liu, Y. Zou, N. Gao, Z. Zhang, Y. Li, Q. Wang, S. Li, and J. Jiang, *J. Am. Chem. Soc.* **136**, 15684–15693 (2014).
- ¹²²S. Fusco, H.-W. Huang, K. E. Peyer, C. Peters, M. Häberli, A. Ulbers, A. Spyrogian, E. Pellicer, J. Sort, S. E. Pratsinis, B. J. Nelson, M. S. Sakar, and S. Pané, *ACS Appl. Mater. Interfaces* **7**, 6803–6811 (2015).
- ¹²³S. Fusco, M. S. Sakar, S. Kennedy, C. Peters, R. Bottani, F. Starsich, A. Mao, G. A. Sotiriou, S. Pané, S. E. Pratsinis, D. Mooney, and B. J. Nelson, *Adv. Mater.* **26**, 952–957 (2014).
- ¹²⁴H. Lee, H. Choi, M. Lee, and P. Sukho, *Biomed. Microdevices* **20**, 103 (2018).
- ¹²⁵A. Y. Rwei, W. Wang, and D. S. Kohane, *Nano Today* **10**, 451–467 (2015).
- ¹²⁶Y. Wang and D. S. Kohane, *Nat. Rev. Mater.* **2**, 17020 (2017).
- ¹²⁷N. M. Idris, M. K. G. Jayakumar, A. Bansal, and Y. Zhang, *Chem. Soc. Rev.* **44**, 1449–1478 (2015).
- ¹²⁸J. Zhuang, R. Wright Carlsen, and M. Sitti, *Sci. Rep.* **5**, 11403 (2015).
- ¹²⁹O. Felfoul, M. Mohammadi, S. Taherkhani, D. de Lanaue, Y. Zhong Xu, D. Loghini, S. Essa, S. Jancik, D. Houle, M. Lafleur, L. Gaboury, M. Tabrizian, N. Kaou, M. Atkin, T. Vuong, G. Batist, N. Beauchemin, D. Radzioch, and S. Martel, *Nat. Nanotechnol.* **11**, 941–947 (2016).
- ¹³⁰H. Li, G. Go, S. Y. Ko, J.-O. Park, and S. Park, *Smart Mater. Struct.* **25**, 027001 (2016).
- ¹³¹J. G. S. Moo, C. C. Mayorga-Martinez, H. Wang, B. Khezri, W. Z. Teo, and M. Pumera, *Adv. Funct. Mater.* **27**, 1604759 (2017).
- ¹³²O. Ergeneman, G. Chatzipirpiridis, J. Pokki, M. Marin-Suárez, G. A. Sotiriou, S. Medina-Rodriguez, J. F. F. Sanchez, A. Fernandez-Gutiérrez, S. Pane, and B. J. Nelson, *IEEE Trans. Biomed. Eng.* **59**, 3104–3109 (2012).
- ¹³³O. Ergeneman, G. Dogangil, M. P. Kummer, J. J. Abbott, M. K. Nazeeruddin, and B. J. Nelson, *IEEE Sens. J.* **8**, 29–37 (2008).
- ¹³⁴“Incorporating in-situ force sensing capabilities in a magnetic microrobot,” in *2014 IEEE/RSJ International Conference on Intelligent Robots and Systems*, edited by W. Jing and D. J. Cappelleri (2014).

- ¹³⁵T. Kawahara, M. Sugita, M. Hagiwara, F. Arai, H. Kawano, I. Shihira-Ishikawa, and A. Miyawaki, *Lab Chip* **13**, 1070–1078 (2013).
- ¹³⁶L. Kong, J. Guan, and M. Pumera, *Curr. Opin. Electrochem.* **10**, 174–182 (2018).
- ¹³⁷H. Ceylan, I. C. Yasa, O. Yasa, A. F. Tabak, J. Giltinan, and M. Sitti, *ACS Nano* **13**, 3353–3362 (2019).
- ¹³⁸S. Lee, S. Kim, S. Kim, J.-Y. Kim, C. Moon, B. J. Nelson, and H. Choi, *Adv. Healthcare Mater.* **7**, e1700985 (2018).
- ¹³⁹D. Jang, J. Jeong, H. Song, and S. K. Chung, *J. Micromech. Microeng.* **29**, 053002 (2019).
- ¹⁴⁰J. Li, X. Li, T. Luo, R. Wang, C. Liu, S. Chen, D. Li, J. Yue, S.-H. Cheng, and D. Sun, *Sci. Rob.* **3**, eaat8829 (2018).
- ¹⁴¹S. Jeon, S. Kim, S. Ha, S. Lee, E. Kim, S. Y. Kim, S. H. Park, J. H. Jeon, S. W. Kim, and C. Moon, *Sci. Rob.* **4**, eaav4317 (2019).
- ¹⁴²K. Malachowski, J. Breger, H. R. Kwag, M. O. Wang, J. P. Fisher, F. M. Selaru, and D. H. Gracias, *Angew. Chem. Int. Ed Engl.* **53**, 8045–8049 (2014).
- ¹⁴³H. Jia, E. Mailand, J. Zhou, Z. Huang, G. Dietler, J. M. Kolinski, X. Wang, and M. S. Sakar, *Small* **15**, 1803870 (2019).
- ¹⁴⁴X. Wang, H. Huang, H. Liu, F. Rehfeldt, X. Wang, and K. Zhang, *Macromol. Chem. Phys.* **220**, 1800562 (2019).
- ¹⁴⁵J.-C. Kuo, H.-W. Huang, S.-W. Tung, and Y.-J. Yang, *Sens. Actuators, A* **211**, 121–130 (2014).
- ¹⁴⁶J. C. Breger, C. Yoon, R. Xiao, H. R. Kwag, M. O. Wang, J. P. Fisher, T. D. Nguyen, and D. H. Gracias, *ACS Appl. Mater. Interfaces* **7**, 3398–3405 (2015).
- ¹⁴⁷J. Kim, A. S. Campbell, B. E.-F. d. Ávila, and J. Wang, *Nat. Biotechnol.* **37**, 389 (2019).
- ¹⁴⁸A. Zuber, E. Klantsataya, and A. Bachhuka, “Biosensing,” *Comprehensive Nanoscience and Nanotechnology*, 2nd ed. (Elsevier, 2019), pp. 105–126.
- ¹⁴⁹D.-H. Kim, P. K. Wong, J. Park, A. Levchenko, and Y. Sun, *Annu. Rev. Biomed. Eng.* **11**, 203–233 (2009).
- ¹⁵⁰X. Yang, T. Zhou, T. J. Zwang, G. Hong, Y. Zhao, R. D. Viveros, T.-M. Fu, T. Gao, and C. M. Lieber, *Nat. Mater.* **18**, 510 (2019).
- ¹⁵¹L. Luan, X. Wei, Z. Zhao, J. J. Siegel, O. Potnis, C. A. Tuppen, S. Lin, S. Kazmi, R. A. Fowler, and S. Holloway, *Sci. Adv.* **3**, e1601966 (2017).
- ¹⁵²J. Li and D. J. Mooney, *Nat. Rev. Mater.* **1**, 16071 (2016).
- ¹⁵³A. S. Hoffman, *Artif. organs* **19**, 458–467 (1995).
- ¹⁵⁴F. Qiu, R. Mhanna, L. Zhang, Y. Ding, S. Fujita, and B. J. Nelson, *Sens. Actuators, B* **196**, 676–681 (2014).
- ¹⁵⁵J.-W. Han, Y. J. Choi, S. Cho, S. Zheng, S. Y. Ko, J.-O. Park, and S. Park, *Sens. Actuators, B* **224**, 217–224 (2016).
- ¹⁵⁶H. Holback, Y. Yeo, and K. Park, “Hydrogel swelling behavior and its biomedical applications,” in *Biomedical Hydrogels*, Woodhead Publishing Series in Biomaterials, edited S. Rimmer (Woodhead Publishing, 2011), Chap. 1, pp. 3–24.
- ¹⁵⁷N. A. Peppas, P. Bures, W. Leobandung, and H. Ichikawa, *Eur. J. Pharm. Biopharm.* **50**, 27–46 (2000).
- ¹⁵⁸L. Vannozzi, I. C. Yasa, H. Ceylan, A. Mencias, L. Ricotti, and M. Sitti, *Macromolecular Bioscience* **18**, 1700377 (2018).
- ¹⁵⁹I. C. Yasa, A. F. Tabak, O. Yasa, H. Ceylan, and M. Sitti, *Adv. Funct. Mater.* **29**, 1808992 (2019).
- ¹⁶⁰S. Balasubramanian, D. Kagan, C. M. Jack Hu, S. Campuzano, M. J. Lobo-Castañón, N. Lim, D. Y. Kang, M. Zimmerman, L. Zhang, and J. Wang, *Angew. Chem.* **123**, 4247–4250 (2011).
- ¹⁶¹J. Goding, C. Vallejo-Giraldo, O. Syed, and R. Green, *J. Mater. Chem. B* **7**, 1625–1636 (2019).
- ¹⁶²D. F. Williams, *Biomaterials* **29**, 2941–2953 (2008).
- ¹⁶³*Foreign Body Reaction to Subcutaneous Implants 2015*, edited by M. Kastellorizos, N. Tipnis, and D. J. Burgess (Springer International Publishing, 2015).
- ¹⁶⁴J. M. Anderson, *Annu. Rev. Mater. Res.* **31**, 81–110 (2001).
- ¹⁶⁵J. M. Morais, F. Papadimitrakopoulos, and D. J. Burgess, *AAPS J.* **12**, 188–196 (2010).
- ¹⁶⁶R. Klopffleisch and F. Jung, *J. Biomed. Mater. Res., Part A* **105**, 927–940 (2017).
- ¹⁶⁷A. Vishwakarma, N. S. Bhise, M. B. Evangelista, J. Rouwkema, M. R. Dokmeci, A. M. Ghaemmaghami, N. E. Vrana, and A. Khademhosseini, *Trends Biotechnol.* **34**, 470–482 (2016).
- ¹⁶⁸H. Yuk, B. Lu, and X. Zhao, *Chem. Soc. Rev.* **48**, 1642–1667 (2019).
- ¹⁶⁹R. Feiner and T. Dvir, *Nat. Rev. Mater.* **3**, 17076 (2018).
- ¹⁷⁰K. C. Spencer, J. C. Sy, K. B. Ramadi, A. M. Graybiel, R. Langer, and M. J. Cima, *Sci. Rep.* **7**, 1952 (2017).
- ¹⁷¹A. A. Sharkawy, B. Klitzman, G. A. Truskey, and W. M. Reichert, *J. Biomed. Mater. Res.* **37**, 401–412 (1997).
- ¹⁷²W. K. Ward, E. P. Slobodzin, K. L. Tiekotter, and M. D. Wood, *Biomaterials* **23**, 4185–4192 (2002).
- ¹⁷³E. R. Aurand, K. J. Lampe, and K. B. Bjurstad, *Neurosci. Res.* **72**, 199–213 (2012).
- ¹⁷⁴J. L. Ifkovits, J. J. Devlin, G. Eng, T. P. Martens, G. Vunjak-Novakovic, and J. A. Burdick, *ACS Appl. Mater. Interfaces* **1**, 1878–1886 (2009).
- ¹⁷⁵J. Kim, M. Dadsetan, S. Ameenuddin, A. J. Windebank, M. J. Yaszemski, and L. Lu, *J. Biomed. Mater. Res., Part A* **95**, 191–197 (2010).
- ¹⁷⁶O. Veisheh, J. C. Doloff, M. Ma, A. J. Vegas, H. H. Tam, A. R. Bader, J. Li, E. Langan, J. Wyckoff, W. S. Loo, S. Jhunjunwala, A. Chiu, S. Siebert, K. Tang, J. Hollister-Lock, S. Aresta-Dasilva, M. Bochenek, J. Mendoza-Elias, Y. Wang, M. Qi, D. M. Lavin, M. Chen, N. Dholakia, R. Thakrar, I. Lacik, G. C. Weir, J. Oberholzer, D. L. Greiner, R. Langer, and D. G. Anderson, *Nat. Mater.* **14**, 643–651 (2015).
- ¹⁷⁷C. Majidi, *Adv. Mater. Technol.* **4**, 1800477 (2019).
- ¹⁷⁸L. Rao, H. Zhou, T. Li, C. Li, and Y. Y. Duan, *Acta Biomater.* **8**, 2233–2242 (2012).
- ¹⁷⁹L. Shi, L. Wang, Y. Duan, W. Lei, Z. Wang, J. Li, X. Fan, X. Li, S. Li, and Z. Guo, *PLoS One* **8**, e55015 (2013).
- ¹⁸⁰P. Calvert, *Adv. Mater.* **21**, 743–756 (2009).
- ¹⁸¹S. P. Lacour, G. Courtine, and J. Guck, *Nat. Rev. Mater.* **1**, 16063 (2016).
- ¹⁸²I. R. Mineev, P. Musienko, A. Hirsch, Q. Barraud, N. Wenger, E. M. Moraud, J. Gandar, M. Capogrosso, T. Milekovic, L. Asboth, R. F. Torres, N. Vachicouras, Q. Liu, N. Pavlova, S. Duis, A. Larmagnac, J. Vörös, S. Micera, Z. Suo, G. Courtine, and S. P. Lacour, *Science* **347**, 159 (2015).
- ¹⁸³L. R. Madden, D. J. Mortisen, E. M. Sussman, S. K. Dupras, J. A. Fugate, J. L. Cuy, K. D. Hauch, M. A. Laflamme, C. E. Murry, and B. D. Ratner, *Proc. Natl. Acad. Sci. U. S. A.* **107**, 15211–15216 (2010).
- ¹⁸⁴B. D. Ratner, *Regener. Biomater.* **3**, 107–110 (2016).
- ¹⁸⁵E. M. Sussman, M. C. Halpin, J. Muster, R. T. Moon, and B. D. Ratner, *Ann. Biomed. Eng.* **42**, 1508–1516 (2014).
- ¹⁸⁶J. M. Anderson and M. S. Shive, *Adv. Drug Delivery Rev.* **28**, 5–24 (1997).
- ¹⁸⁷M. Patenaude and T. Hoare, *ACS Macro Lett.* **1**, 409–413 (2012).
- ¹⁸⁸B. F. Matlaga, L. P. Yashchak, and T. N. Salthouse, *J. Biomed. Mater. Res.* **10**, 391–397 (1976).
- ¹⁸⁹T. N. Salthouse, *J. Biomed. Mater. Res.* **18**, 395–401 (1984).
- ¹⁹⁰A. S. Thakor, J. V. Jokerst, P. Ghanouni, J. L. Campbell, E. Mittra, and S. S. Gambhir, *J. Nucl. Med.* **57**, 1833–1837 (2016).
- ¹⁹¹M. Mahmoudi, H. Hofmann, B. Rothen-Rutishauser, and A. Petri-Fink, *Chem. Rev.* **112**, 2323–2338 (2012).
- ¹⁹²D.-I. Kim, H. Lee, S.-H. Kwon, H. Choi, and S. Park, *Sens. Actuators, B* **289**, 65–77 (2019).
- ¹⁹³B. Jang, E. Gutman, N. Stucki, B. F. Seitz, P. D. Wendel-García, T. Newton, J. Pokki, O. Ergeneman, S. Pané, and Y. Or, *Nano Lett.* **15**, 4829–4833 (2015).
- ¹⁹⁴M. Dai, R. Jungmann, and P. Yin, *Nat. Nanotechnol.* **11**, 798 (2016).
- ¹⁹⁵H. Wang and M. Pumera, *Chem. Rev.* **115**, 8704–8735 (2015).
- ¹⁹⁶O. Vermesh, A. Aalipour, T. J. Ge, Y. Saenz, Y. Guo, I. S. Alam, S.-M. Park, C. N. Adelson, Y. Mitsutake, J. Vilches-Moure, E. Godoy, M. H. Bachmann, C. C. Ooi, J. K. Lyons, K. Mueller, H. Arami, A. Green, E. I. Solomon, S. X. Wang, and S. S. Gambhir, *Nat. Biomed. Eng.* **2**, 696 (2018).
- ¹⁹⁷S. M. Azarin, J. Yi, R. M. Gower, B. A. Aguado, M. E. Sullivan, A. G. Goodman, E. J. Jiang, S. S. Rao, Y. Ren, S. L. Tucker, V. Backman, J. S. Jeruss, and L. D. Shea, *Nat. Commun.* **6**, 8094 (2015).
- ¹⁹⁸S. S. Rao, G. G. Bushnell, S. M. Azarin, G. Spicer, B. A. Aguado, J. R. Stoehr, E. J. Jiang, V. Backman, L. D. Shea, and J. S. Jeruss, *Cancer Res.* **76**, 5209–5218 (2016).
- ¹⁹⁹X. Yan, Q. Zhou, J. Yu, T. Xu, Y. Deng, T. Tang, Q. Feng, L. Bian, Y. Zhang, and A. Ferreira, *Adv. Funct. Mater.* **25**, 5333–5342 (2015).

- ²⁰⁰J. Park, C. Jin, S. Lee, J. Y. Kim, and H. Choi, *Adv. Healthcare Mater.* **8**, 1900213 (2019).
- ²⁰¹K. Kobayashi, C. Yoon, S. H. Oh, J. V. Pagaduan, and D. H. Gracias, *ACS Appl. Mater. Interfaces* **11**, 151–159 (2018).
- ²⁰²“On the role of machine learning algorithms in developing MEMS components,” in *Proceedings International Conference on MEMS, NANO and Smart Systems*, edited by D. Asmar, M. Moussa, and J. Zelek (IEEE, 2003).
- ²⁰³“Machine learning based fitness tracker platform using MEMS accelerometer,” in *2017 International Conference on Computer, Electrical & Communication Engineering (ICCECE)*, edited by Y. Jain, D. Chowdhury, and M. Chattopadhyay (IEEE, 2017).
- ²⁰⁴M. L. Giger, *J. Am. Coll. Radiol.* **15**, 512–520 (2018).
- ²⁰⁵L. Alvarez, B. M. Friedrich, G. Gompper, and U. B. Kaupp, *Trends Cell Biol.* **24**, 198–207 (2014).